112

Forecasting Research

Scientific Note No. 23

THE NON-LINEAR EVOLUTION OF A SLOWLY GROWING WAVE ON A LATERALLY SHEARED BAROCLINIC FLOW

by
M.J. Bell

April 1991

ORGS UKMO S Duplicate

National Meteorological Library
FitzRoy Road, Exeter, Devon. EX1 3PB

Meteorological Office (Met O 11)
London Road, Bracknell, Berkshire RG12 2SZ, England

Short-Range Forecasting Research Scientific Note No. 23

THE NON-LINEAR EVOLUTION OF A SLOWLY GROWING WAVE ON A LATERALLY SHEARED BAROCLINIC FLOW

by

M. J. Bell

April 1991

Short-Range Forecasting Division
The Met. Office
London Rd.
Bracknell
Berkshire RG12 2SZ
ENGLAND

N. B. This paper has not been published. Permission to quote from it must be obtained from the Assistant Director of the above Met. Office division.

THE NON-LINEAR EVOLUTION OF A SLOWLY GROWING WAVE ON A LATERALLY SHEARED BAROCLINIC FLOW

M. J. Bell

April 1991

Short-Range Forecasting Division, Room H021, Hadley Centre,
U. K. Met. Office, London Rd., Bracknell, RG12 2SZ

ABSTRACT

Wave disturbances to baroclinic flows produce cyclones in the atmosphere and eddies in the oceans and have been extensively studied in laboratory experiments with differentially heated annuli of rotating fluid. Related analytical studies have concentrated mainly on the development of slowly growing waves on laterally uniform zonal flows. Neutral inviscid waves on such flows do not advect their own potential vorticity (p.v.) field whereas neutral waves on most laterally sheared baroclinic flows do. Scaling arguments suggest that on these laterally sheared flows the harmonics generated by the neutral waves play the dominant role in arresting the initial growth of weakly unstable waves. The arrest of a wave is chiefly accomplished by fully non-linear advection within a critical layer centred on the wave's steering level whose depth is proportional to the wave's amplitude.

Explicit numerical solutions illustrating these points are presented for a case in which the critical level is non-singular and the inviscid calculations comparatively straightforward. The stability of the solutions and the effects of diffusive fluxes on them are discussed. Scale analysis of processes neglected in the calculations suggests that they may be most relevant to the interpretation of annulus experiments with fluids of high Prandtl number near the upper axisymmetric transition (UAT). P.v. diagnostics for a numerical simulation near the UAT indicate that distortion of the wave's p.v. field is mainly confined to the vicinity of the steering level in a manner consistent with the inviscid calculations.

1. INTRODUCTION

The growth and equilibration of mid-latitude weather systems is a subtle phenomenon. Some insight into it was gained by Charney (1947) and Eady (1949) who investigated the stability of baroclinic zonal flows to waves of small amplitude growing without changing shape (i.e. of normal mode form), a problem which contains some of the essential physics of the phenomenon in a form which is amenable to mathematical analysis. Later, Charney and Stern (1962) and Pedlosky (1964) developed the quasi-geostrophic equations which provide the most convenient mathematical framework for the analytical study of the initial growth of cyclones. According to these equations (see e.g. Pedlosky 1982a) the fluid motions are governed by the boundary conditions and the conservation of the quasi-geostrophic potential vorticity q following the geostrophic motion:

$$q_t + J(\psi, q) = 0 \tag{1.1}$$

$$\text{where } q = f + \psi_{xx} + \psi_{yy} + (\psi_z / B)_z . \tag{1.2}$$

Here ψ is the streamfunction of the geostrophic velocity, subscripts denote partial derivatives and $J(a, b) = a_x b_y - a_y b_x$ is the Jacobian derivative. Variables have been non-dimensionalised in the standard manner and B, the Burger number, is given by

$$B = N^2H^2 / f^2L^2 \tag{1.3}$$

where f is the Coriolis parameter, N the Brunt-Vaisala frequency, and H the vertical and L the horizontal length scales used in the non-dimensionalisation.

Provided the boundary conditions are inviscid, any steady zonal flow U(y,z) is an exact solution of (1.1) and the evolution of a perturbation ψ' to U is governed by

$$q'_t + U q'_x + Q_y \psi'_x + J(\psi', q') = 0 \tag{1.4}$$

where Q_y denotes the lateral gradient of the potential vorticity of the basic zonal flow and q' the potential vorticity of the perturbation. The stability of U(y,z) to very small wave-like perturbations of constant shape

$$\psi' = Re\{\phi(y,z)\, exp ik(x - ct)\} \tag{1.5}$$

is hence determined by the well known equation

$$(U - c)q' + Q_y\psi' = 0 \tag{1.6}$$

and its boundary conditions.

Under inviscid boundary conditions the Burger number is the only non-dimensional combination of the imposed conditions on which the solutions of equations (1.1) and (1.6) depend. The evolution governed by (1.1) of waves growing from small amplitude is most easily studied at Burger numbers close to a value, B_0 say, at which there is a neutrally stable wave with streamfunction ψ_s and real phase speed c_s. The initial growth rate of such waves and the amplitude to which they grow then tends to be small. Consequently the advection of the wave by the zonal flow usually dominates that by the wave itself. Where

this is the case the streamfunction can usefully be expressed as a summation,

$$\psi' = \sum_{n=1} \delta^n \psi_n \,, \tag{1.7}$$

in which δ is B_0 - B raised to a suitable (positive) power (Pedlosky 1970 , Drazin 1970). The equations governing the wave's evolution can be reduced to a series of forced linear problems

$$(U - c) q_n + Q_y \psi_n = R_n \tag{1.8}$$

(cf (1.6)) in which R_n is an expression which includes only terms ψ_m and q_m with $m < n$.

Since close to B_0 the streamfunction ψ' of the growing wave is dominated by the streamfunction ψ_s of the neutral mode itself, the (non-linear) self-interaction of the slowly growing wave, $J(\mathrm{Re}\,\psi', \mathrm{Re}\,q')$, is dominated by

$$J(Re\,\psi_s, Re\,q') = -J(Re\,\psi_s, Re\{Q_y \psi_0 / (U - c)\}) \tag{1.9a}$$

$$= -Re\,\psi_{sx} Re\{\psi_s\, \partial / \partial y (Q_y / (U - c))\} + \frac{Q_y c_i}{|U-c|^2} J(Re\,\psi_s, Im\,\psi_s) \tag{1.9b}$$

The first equality above follows from (1.6) and the second from the definition of the Jacobian. The discussion of this equation in the next three paragraphs contains the main points of the paper.

The first of the two terms on the r.h.s. of (1.9b) is identically zero for waves on laterally uniform flows U(z) and non zero at most locations in the meridional plane for most laterally sheared zonal flows U(y,z). The second term is also identically zero for any neutral mode subject to inviscid boundary conditions, for such neutral modes may be taken to be purely real-valued. Thus the dominant non-linear interaction for inviscid waves depends significantly on the lateral shear of the zonal flow.

Neutral modes subject to Ekman pumping have vertical phase shifts and complex-valued streamfunctions. Hence the second term on the r.h.s. of (1.9b) can be non-zero for these modes and represents the dominant non-linear interaction on laterally uniform flows. It is doubtful, however, that diffusive fluxes in the interior can be consistently neglected for such waves, particularly in view of the fact that Q_y need not be zero at their steering levels. The evolution of waves which are subject to Ekman pumping is not considered in detail below for this reason.

Close to the steering level of a slowly growing inviscid wave on a laterally sheared flow, where U is equal to c_s and $q'_t + U\,q'_x \equiv (U - c_s) q'_x$ is small, the non-linear advection (the first term on the r.h.s. of (1.9b))dominates the growth rate and linear advection of q. From (1.4) and (1.9) it is clear that this is true whether $Q_y / (U - c_s)$ is bounded at the critical level or not. The self-advection of the wave is of the same order of magnitude as the advection by the zonal flow within a region of depth directly proportional to the amplitude of the wave. Within this region, in a time which is inversely proportional to the amplitude of the wave's streamfunction, many zonal harmonics of the wave's potential vorticity field are excited to amplitudes of the same order of magnitude as that of the potential vorticity of the fundamental. Outside this layer, the self advection generates only the first harmonic of the wave at an amplitude comparable with the square of the amplitude, A, of the fundamental

wave (i.e. of $O(A^2)$). Advection of this harmonic by the fundamental produces corrections to the fundamental only of $O(A^3)$.

In order to show that the evolution of the wave as a whole is determined by the advection within the (narrow) critical layer rather than in the bulk of the interior or at the boundaries, the boundary conditions must be considered. We assume that the fluid is confined within horizontal boundaries at $z = -½ , ½$ and vertical boundaries at $y = 0 , 1$ through which there is no normal motion. When combined with the thermodynamic equation and the Ekman pumping formula the absence of vertical velocity at the horizontal boundaries yields

$$\psi_{zt} + J(\psi,\psi_z) = \pm\epsilon(\psi_{xx} + \psi_{yy}) \quad at\, z = \pm ½ . \tag{1.10}$$

The precise value of the Ekman pumping parameter is not important here. In the presence of Ekman pumping steady zonal flows with lateral variation generally do not satisfy this condition. For flows that do (e.g. any flow in the absence of Ekman pumping) repetition of the analysis of (1.4) - (1.8) yields

$$(U - c_s)\psi_{nz} - U_z\psi_n \pm i\epsilon(\psi_{nxx} + \psi_{nyy}) = S_n \tag{1.11}$$

where S_n is the counterpart of R_n in (1.8).

Provided the steering level is not near the boundaries the main self interaction of the growing wave there is

$$J(Re\psi_s, Re\psi_{sz}) = J(Re\psi_s, \frac{U_z}{U-c_s} Re\psi_s \pm \frac{\epsilon}{U-c_s} Im\ \nabla_h^2\psi_s) \tag{1.12}$$

$$= Re\,\psi_s\, Re\,\psi_{sx}\partial/\partial y\{(U_z/U - c_s)\} \pm \epsilon J(Re\,\psi_s, Im\{\frac{\nabla_h^2\psi_s}{(U-c_s)}\})$$

For laterally uniform flows the first term on the r.h.s. of (1.12) is again identically zero and when Ekman pumping is present the vertical variations in the azimuthal phase of the wave, sustaining it against spin-down, give rise to the dominant non-linear interactions, either at the endwalls ((1.12) and Drazin (1972)) or in the interior (see (1.9)). For the more general case of a laterally sheared zonal flow, providing the steering level is confined to the flow interior so that zonal advection dominates, the (self induced) boundary forcing generates only the first harmonic of the wave and a correction to the axisymmetric flow at amplitudes of $O(A^2)$). No self induced forcing arises at the side-walls.

Outside the critical layer, the interior equations (1.8) can be interpreted as formulae for the vertical derivative of ψ'_z whose values at the upper and lower boundaries are constrained by (1.11). The influence of the critical layer on the flow outside it is determined by the jump in ψ'_z across it. Within the critical layer q' is at least of O(A) and variation of the horizontal advection of q' with height will ensure that the stretching term $(\psi'_z / B)_z$ is of the same order as q'. The jump in the fundamental wave's values of ψ'_z across a critical layer whose depth is of O(A) is hence at least of $O(A^2)$. By comparison the non-linear thermal advection at the boundaries (given by (1.12)) can only affect the fundamental wave at $O(A^3)$and the advection of potential vorticity in the bulk of the interior similarly affects the difference between the values of the fundamental of ψ'_z at each boundary only at $O(A^3)$.

We conclude from the above discussion that the arrest of the growth of inviscid waves growing from small amplitude on laterally sheared baroclinic flows is qualitatively different from that on laterally uniform flows and that the evolution on laterally uniform flows is not structurally stable (i.e. it is not robust to the introduction of small lateral variations in the zonal flow). On the laterally sheared flow the lateral structure of the neutral wave is complicated enough for it to advect its own potential vorticity field (see (1.9)). This advection is at least comparable with that by the zonal flow within a layer centred on the neutral mode's steering level whose (non-dimensional) depth is of the same order as the amplitude of the wave. The fully non-linear advection within this narrow layer has a larger effect on the fundamental wave than the non-linear advection at the boundaries or in the rest of the interior and is hence the first to change the linear growth rate of a disturbance growing from small amplitude.

Sections 2 and 3 present detailed calculations illustrating this evolution on an f-plane for the flow

$$U = \tfrac{1}{2}(1 - a_s + a_s \sin \pi y) \sin \pi z \qquad (1.13)$$

which supports neutral normal modes of the form

$$\psi_s = \rho_s(y) \cos kx \quad , \quad c_s = 0 \quad . \qquad (1.14)$$

The calculations are particularly straightforward for this case because $Q_y / (U - c_s)$ is bounded at the steering level and the steering level is horizontal, lying on the plane $z = 0$. In section 2 the domain is divided into a region surrounding the steering level and two outer regions and the solutions in each region matched together. The resulting equation describing the evolution of the wave amplitude and of the potential vorticity in the critical layer is similar to those obtained by Stewartson (1978) and Warn & Warn (1978) and particularly by Warn & Gauthier (1989), but is difficult to solve analytically. Approximate numerical solutions are presented in section 3.

Various features and deficiencies of these solutions are discussed in section 4. These include the stability of the solutions to short wavelength disturbances (Killworth and McIntyre 1985), the importance of singular critical levels, the adequacy of the quasi-geostrophic equations and the influences of diffusive processes. Section 5 discusses the relevance of the work to the flows obtained near the upper axisymmetric transition in the differentially heated rotating annulus experiments (Hide & Mason 1975). This paper developed from attempts to understand these flows, and joint laboratory and numerical investigations of them appear to be the most promising approach to determining whether the processes described here are important in real fluids. Concluding remarks are made in section 6.

2. ANALYSIS OF A NON-LINEAR BAROCLINIC CRITICAL LAYER

Problem Definition

The quasi-geostrophic equations for an f plane will be assumed to govern the motion:

$$Bq_t + J(\psi, Bq) = 0 \ , \quad -\tfrac{1}{2} \le z \le \tfrac{1}{2} \tag{2.1}$$

$$Bq = B(f + \nabla_h^2 \psi) + \psi_{zz} \tag{2.2}$$

$$\psi_{zt} + J(\psi, \psi_z) = 0 \ \ on\ z = \pm\tfrac{1}{2} \tag{2.3}$$

$$\psi_x = 0 \ \ and \ \ \Psi_{yt} = 0 \ \ on\ y = 0, 1 \ . \tag{2.4}$$

(2.1) represents conservation of the quasi-geostrophic potential vorticity (2.2) following the geostrophic motion. (2.3) represents conservation of potential temperature at the horizontal boundaries where the vertical veloctiy vanishes in the absence of Ekman pumping. No normal flow and energy conserving conditions on the zonal mean streamfunction Ψ are applied at the side boundaries (2.4). The stratification is taken to be independent of height and the channel to be periodic in x with non-dimensional repeat length l_s. The zonal flow is assumed to be an internal baroclinic jet (Charney & Stern 1964) of the form

$$U = \tfrac{1}{2} \sin\pi z \, (1 - a_s + a_s \sin\pi y) \ . \tag{2.5}$$

This flow is studied at a Burger number slightly smaller than that at which there is a neutral mode which advects its own potential vorticity field (see (1.9)). The evolution of the only unstable weakly growing normal mode is traced as it grows from a very small initial amplitude.

The form of the neutral normal mode and the appropriate scalings are summarised first. The outer solutions (i.e. those outside the critical layer) are then developed and the jump conditions across the critical layer established. Presentations of the inner solution and the matching of the inner solution with the jump in the outer thermal field across the critical layer follow. Finally formulae are derived for the unstable linear normal mode in the inner and outer regions (which serve as the initial conditions). The key formulae are sumarised at the end of the section.

The potential vorticity fields of the inner and outer solutions will be denoted by p and q respectively and the inner and outer streamfunctions by φ and ψ . P, Q, Φ and Ψ denote the corresponding zonal mean fields.

Neutral mode solution

$B\,Q_y / U$ is well defined for (2.5) and independent of height;

$$BQ_y / U = \pi^2 \ + \ \frac{B\pi^2 a_s \sin\pi y}{1 - a_s + a_s \sin\pi y} \ . \tag{2.6}$$

Direct substitution in (2.1) - (2.4) shows that

$$\psi_s = \rho_s(y)\cos r\pi x \quad with \quad r = 2/l_s \tag{2.7}$$

is a stationary solution ($c_s = 0$) of the quasi-geostrophic equations linearised about the zonal flow (2.5) when ρ_s is the gravest mode solution of

$$\rho_{yy} + \frac{\pi^2 a_s \sin \pi y}{1 - a_s + a_s \sin \pi y}\rho + \lambda\rho = 0, \quad 0 \le y \le 1$$
$$\rho = 0 \ on \ y = 0,1 \ , \tag{2.8}$$

and the Burger number, B, is related to the gravest mode's eigenvalue, λ_s, by

$$B = \frac{\pi^2}{\lambda_s + r^2\pi^2} = B_0 \, . \tag{2.9}$$

This neutral mode solution is clearly non-singular and independent of height. Bell & White (1988) (and Bell 1989) show that the normal mode which springs from this neutral one as B is reduced is the only unstable normal mode at values of B just smaller than B_0.

Scaling considerations

The Burger number is assumed to be just less than B_0;

$$B = B_0 - \Delta B \ . \tag{2.10}$$

As shown by Bell and White (1988) (and in appendix B) the normal mode growth rate is then of $O(\Delta B)$. So we introduce an appropriate slow time τ;

$$\tau = \Delta B \, t \ . \tag{2.11}$$

Harmonics and non-linear corrections to the dominant wave mode are generated by the neutral mode's self advection at a rate of $O(A^2)$, A being the wave amplitude. So the non-linear advection can combat the linear growth if

$$A = \Delta B \, a(\tau) \ , \tag{2.12}$$

$a(\tau)$ being of O(1) when linear growth and non-linear advection become comparable. Since within the critical layer the zonal velocity U of (2.5) is of the order $\pi z/2$, the critical layer has a depth of $O(\Delta B)$ (for $z >> \Delta B$ zonal flow advection dominates). So the stretched vertical ordinate ζ,

$$z = \Delta B \, \zeta \ , \tag{2.13}$$

will be used within the critical layer. The inner solution has domain $-\infty < \zeta < +\infty$ and for $\zeta \to \pm\infty$ must match the outer solutions for $z \to 0^{\pm}$.

Outer solutions

Two outer solutions are required; one above and one below the critical layer. The equations governing the two are very similar and for the most part they will not be painstakingly distinguished. We pose the perturbation expansion for the streamfunction

suggested by (2.12)

$$\psi = \Psi_0 + \Delta B\psi_1 + \Delta B^2\psi_2 + \ldots \tag{2.14}$$

in which Ψ_0 is the streamfunction of the zonal flow (2.5). Substituting into (2.1) and (2.3) and using (2.10) one obtains at O(ΔB):

$$M_0\psi_{1x} \equiv (B_0\,\nabla_h^2 + \partial^2/\partial z^2)\psi_{1x} + (BQ_y/U)_{B=B_0}\psi_{1x} = 0$$
$$\psi_{1zx} = 0 \;\; on\; z = \pm ½ \tag{2.15}$$

So the outer solution to first order is proportional to the gravest mode solution;

$$\psi_1 = \{a(\tau)\cos r\pi x + b(\tau)\sin r\pi x\}\,\rho_s(y)\ . \tag{2.16}$$

Strictly speaking the most general outer solutions should be matched across the critical layer to reach this conclusion; but the depth independent solution (2.16) does satisfy the inner equations at lowest order as will become apparent. An undetermined axisymmetric perturbation should also be retained at this point but examination of the problem at the next order ((2.17) below) shows that it is not excited at this order.

At O(ΔB²) (2.1) divided by U and (2.2) yield

$$M_0\psi_{2x} = -B_0/U\,\nabla_h^2\psi_{1\tau} - J(\psi_1, B_0\,\nabla_h^2\psi_1)/U + U_{zz}\psi_{1x}/(B_0U) \tag{2.17}$$

$$\psi_{2zx} = 0 \;\; on\; z = \pm ½\ . \tag{2.18}$$

The l.h.s of (2.17) involves an elliptic operator (defined in (2.15)) on ψ_{2x} and the r.h.s. terms $-B_0\,q_{1\tau}/U$ and $-J(\psi_1, B_0\,q_1)/U$ which are singular at $z=0$ on the edges of the two domains. The forcing terms on the r.h.s. of (2.17) do not induce any axisymmetric motions as anticipated in (2.16). (2.17) and (2.18) become a well defined problem if jump conditions on ψ_2 and ψ_{2z} across $z=0$ are specified:

$$\left[\psi_2\right]_{0^-}^{0^+} = H(x,y)\ ;\ \left[\psi_{2z}\right]_{0^-}^{0^+} = I(x,y)\ . \tag{2.19}$$

H(x,y) and I(x,y) are understood to depend on the inner solution.

As shown in appendix A, (2.17) - (2.19) have solutions provided

$$\left[\iint \rho_s(y)\exp(ir\pi x)\psi_{2z}\,dxdy\right]_{-z}^{z} \rightarrow \frac{\pi^2}{B_0}\iint \rho_s(y)\exp(ir\pi x)\psi_1\,dxdy \;\; as\; z \downarrow 0\ . \tag{2.20}$$

This (Fredholm type) condition ensures that I(x,y) does not resonantly force (2.17) by projecting onto the unforced neutral solution.

Inner Solution

From (2.2) and (2.13) , the potential vorticity in the critial layer, p, is related to the streamfunction, φ , by

$$Bp = Bf + B\,\nabla_h^2\varphi + \frac{1}{\Delta B^2}\varphi_{\zeta\zeta} . \tag{2.21}$$

The conservation of potential vorticity, (2.1), is expressed by

$$\Delta B\{Bp_\tau + J(\varphi, Bp)\} = 0 . \tag{2.22}$$

We pose a series expansion for φ in powers of ΔB;

$$\varphi = \Delta B\,\varphi_1 + \Delta B^2\,\varphi_2 + \Delta B^3\,\varphi_3 + \ldots\ldots \tag{2.23}$$

For $\zeta \to \pm\infty$, φ must match to the outer solution with $z \to 0^{\pm}$ which is given to $O(\Delta B)$ by

$$\psi_{out} = \Delta B\{\pi\zeta\,/\,2 - \Delta B^2(\pi\zeta)^3\,/\,12 + O(\Delta B^4)\}\{-(1-a_s)y + a_s\,/\,\pi\,\cos\pi y\}$$
$$+ \Delta B(a(\tau)\cos r\pi x + b(\tau)\sin r\pi x)\rho_s(y) + O(\Delta B^2) . \tag{2.24}$$

The terms of $O(\Delta B^3)$ in (2.24) describe the initial zonal mean flow to $O(\Delta B^3)$. They are included for reference in the derivation of (2.31) below.

<u>At O(1)</u>, (2.22) is

$$\varphi_{1\zeta\zeta\tau} + J(\varphi_1, \varphi_{1\zeta\zeta}) = 0 . \tag{2.25}$$

A (barotropic wave) solution which matches to the outer is

$$\varphi_1 = -\frac{\pi\zeta}{2}\{(1-a_s)y - \frac{a_s}{\pi}\cos\pi y\} + \rho_s(a(\tau)\cos r\pi x + b(\tau)\sin r\pi x) . \tag{2.26}$$

The mean flow in the outer is time independent so $\Phi_{1\tau} = 0$.

<u>At O(ΔB)</u>, (2.22) is

$$\varphi_{2\zeta\zeta\tau} + J(\varphi_1, \varphi_{2\zeta\zeta}) = 0 . \tag{2.27}$$

The partial solution

$$\varphi_2 = \Phi_2(y,\zeta) + \sum_{k,l}(c^{(k,l)}\cos rk\pi x + d^{(k,l)}\sin rk\pi x)\rho^{(k,l)}(y) \tag{2.28}$$

is in fact adequate. Solutions with $\varphi_{2\zeta\zeta}$ non-zero would require potential vorticity gradients of O(1) which cannot develop for ζ of O(1) since p is conserved by the horizontal geostrophic motion. (Such solutions are probably important in the development of flows with singular critical levels.) Wave solutions directly proportional to ζ are not required because the O(ΔB) outer streamfunction (2.16) is barotropic (i.e. $\psi'_z = 0$).

At O(ΔB^2), the highest order considered here, (2.22) is

$$p_{1\tau} + J(\varphi_1, p_1) = 0 \tag{2.29}$$

where

$$Bp_1 = B_0 \nabla_h^2 \varphi_1 + \varphi_{3\zeta\zeta} \ . \tag{2.30}$$

(2.29) and (2.30) assert that the O(ΔB) potential vorticity, p_1, is conserved following the O(ΔB) geostrophic motion. Using (2.24) one finds that the zonal flow by itself initially has

$$BP_1 = \frac{\pi^3\zeta}{2}\{(1-a_s)y - (1+B_0)\frac{a_s}{\pi}\cos\pi y\} \ . \tag{2.31}$$

The inviscid boundary conditions (2.4) imply that $\varphi'_3 = 0$ on y = 0,1 and (2.26) with (2.8) implies that $\varphi'_{1yy} = 0$ on $y = 0,1$ so

$$p'_1 = 0 \ on \ y = 0, 1 \ . \tag{2.32}$$

Furthermore $\Phi_{1y\tau} = 0$ and $\Phi_{3y\tau} = 0$ on $y = 0,1$. For a pure wave perturbation $\Phi_3 = 0$ at time $\tau = 0$ so using (2.31)

$$BP_{1y} = \pi^3\zeta(1-a_s)/2 \ on \ y = 0, 1 \ . \tag{2.33}$$

Matching condition

For the inner, φ, and outer, ψ, solutions to match, they and their derivatives must agree over an intermediate ranges of depths $z_a < z_o < z_b$ in which $z_o/\Delta B \to \infty$ and $z_o \to 0$ as $\Delta B \to 0$. Within this range of depths we thus require

$$\left[\psi'_z\right]_{z=-z_0}^{z=+z_0} = \left[1/\Delta B \ \varphi'_\zeta\right]_{\zeta=-z_0/\Delta B}^{\zeta=z_0/\Delta B} \quad as \ \Delta B \to 0 \ . \tag{2.34}$$

For the solutions presented above, to O(ΔB^2) (2.34) is

$$\Delta B^2 \left[\psi'_{2z}\right]_{z=0^-}^{z=0^+} = \Delta B^2 \int_{\zeta=-\infty}^{\zeta=+\infty} \varphi'_{3\zeta\zeta} \, d\zeta \ . \tag{2.35}$$

Using (2.35), the solvability condition (2.20) can be expressed as

$$\int_{-\infty}^{+\infty} \iint \rho_s exp(ir\pi x)\varphi_{3\zeta\zeta} dx \, dy \, d\zeta = \frac{\pi^2}{B_0} \iint \rho_s exp(ir\pi x)\psi_1 \, dx \, dy \ . \tag{2.36}$$

Initial conditions

An appropriate initial condition for the perturbation streamfunction is that of the linearly unstable normal mode (though see Warn & Gauthier 1989). As shown in appendix B the normal mode with an initial outer streamfunction of small amplitude γ

$$\varphi_1' = \gamma \cos(r\pi x)\,\rho_s(y) \tag{2.37}$$

has accompanying vertical variation

$$\varphi_{3\zeta\zeta}' = \frac{\gamma B_0 (Q_y/U)\rho_s}{|\tilde{U}-c|^2}\{\,|c|^2 \cos(r\pi x) + \tilde{U}|c|\sin(r\pi x)\} \tag{2.38}$$

in the critical layer. In (2.38)

$$\tilde{U} = \frac{\Delta B \pi \zeta}{2}(\,1 - a_s + a_s \sin \pi y\,) \quad and \quad c = \frac{i\Delta B T}{2B_0^2} \tag{2.39}$$

$$with\ T = \frac{\int \pi^2 \rho_s^2\, dy}{\int \rho_s^2 (Q_y/U)(1-a_s+a_s \sin \pi y)^{-1}\, dy}. \tag{2.40}$$

Summary

The above analysis treats the development of a wave which starts as a slowly growing normal mode disturbance of small amplitude on a baroclinic zonal flow which has Q_y=U=0 on z=0 (see (2.5)). It is set at a Burger number, B_0-ΔB, where this wave is the only linearly unstable normal mode. The wave is governed by its evolution in a critical layer with a depth of O(ΔB) and grows to an amplitude of O(ΔB). Its streamfunction to O(ΔB) is barotropic both inside and outside the critical layer (see (2.26) and (2.16)) and has the same spatial form as the neutral normal mode (2.7). The O(ΔB) potential vorticity within the critical layer, p_1 as defined by (2.30), is conserved following the O(ΔB) geostrophic motion (2.29). Boundary conditions on p_1 are provided by (2.32) and (2.33) and the amplitudes $a(\tau)$ and $b(\tau)$ of the O(ΔB) wave streamfunction are determined by the constraint (2.36) which ensures that the jump in the thermal field across the critical layer (resulting from potential vorticity advection within it) does not resonantly force the neutral normal mode outside the critical layer. Since (2.36) is satisfied by the initial conditions it is adequate to satisfy only its time derivative with respect to τ. Expressing $\varphi_{3\zeta\zeta\tau}$ in terms of $J(\varphi_1, Bp_1)$ and φ_1 by using (2.29) and (2.30), the time derivative of (2.36) yields

$$-\int_\zeta \iint \rho_s \exp(ir\pi x) J(\varphi_1, B_0 p_1)\, dydz =$$

$$\iint \frac{\pi^2}{B_0}\rho_s^2 \exp(ir\pi x)\,\{a_\tau \cos(r\pi x) + b_\tau \sin(r\pi x)\}\, dx\, dy \tag{2.41}$$

$$-\int_\zeta \iint B_0 (Q_y / U)\,\rho_s^2 \exp(ir\pi x)\,\{a_\tau \cos(r\pi x) + b_\tau \sin(r\pi x)\}\, dx\, dy d\zeta\,.$$

Thus the evolution is determined by (2.29) with φ_1 given by (2.26), which must be solved subject to (2.32), (2.33) and (2.41).

3. NUMERICAL SOLUTIONS

Method

Numerical solutions for the potential vorticity in the inner region have been obtained using a gridpoint model with variable vertical and horizontal resolution. On the IZth level a uniform grid is employed with IXP(IZ) points along-stream and IYP(IZ) points within the channel across-stream. The cross-stream gridpoints straddle the boundaries y=0,1 and conditions (2.32) and (2.33) are applied using second order accurate formulae. Forward steps of (2.29) are performed by the leapfrog method with the source function $J(\varphi_1, p_1)$ evaluated according to Arakawa's energy and enstrophy conserving formula (Haltiner & Williams 1980). Explicit horizontal diffusion is invoked to dampen small scales, so that in place of (2.29) the equation being integrated is

$$p_{1\tau} = -J(\varphi_1, p_1) + \nu_d \nabla_h^2 p_1 - \nu_b \nabla_h^4 p_1 \equiv S_1 \ . \tag{3.1}$$

Standard four point formulae are used for the Laplacian operators and the additional homogeneous boundary condition

$$\nabla_h^2 p_1 = 0 \ on \ y = 0,1 \tag{3.2}$$

is used when ν_b is non-zero. A very weak Robert filter with coefficient R_f is employed to dampen the computational mode; the resulting error in the source function is

$$\Delta S_1 = p_{1\tau\tau} \Delta\tau^2 R_f \ , \tag{3.3}$$

$\Delta\tau$ being the timestep. In all integrations the initial forward step is specified to be one eighth of the standard length and Miyakoda's method (Hoskins and Simmons 1975) used to reach the standard step length.

In the experiments reported here, for $-2c_1 < \zeta < 2c_1$ (i.e. close to the steering level) the vertical spacing (DZ1) and horizontal spacing are independent of depth and ζ=0 is chosen to be one of the levels. The numbers of points along- and across-stream in this region are denoted by IXPTS and IYPTS respectively. In order to obtain an r% relative error in the initial growth rate, the depth of the domain, h, must be great enough that the critical layer integral

$$I(h) = \int_{-h}^{+h} \frac{c_1}{(\zeta^2 + c_1^2)} d\zeta = 2 \arctan(h / c_1) \tag{3.4}$$

is within r% of I(h=∞). For a 5% error in I(h) we need $h > 16\ c_1$. Manipulation of standard formulae bounding the error in evaluations of I by the trapezoidal rule (Kreyszig 1982) suggests that a uniform distribution of errors is obtained at large values of $|\zeta|$ by taking the spacing to be proportional to $|\zeta|^{4/3}$. The spacing is specified to grow at this rate for $|\zeta| > 2c_1$.

Since the zonal flow is proportional to ζ , for large values of $|\zeta|$ the zonal flow is very strong. In order to satisfy the CFL stability criterion the horizontal resolution must decrease with $1/|\zeta|$, or the time step be inversely proportional to the height of the top level. Since good horizontal resolution is only required near the steering level the former option is used

and for $|\zeta| > 2c$

$$IXP(IZ) = IXPTS / (|\zeta| (IZ) / 2c_1) \ . \tag{3.5}$$

IYP(IZ) varies similarly with ζ. Equation (2.41) is evaluated using standard formulae with the source function on the left hand side given by (3.1) (i.e. it includes the diffusive fluxes).

In order to reduce the computational cost, advantage was taken of symmetries of the solution which are present in the initial conditions and retained by the governing equations. Consider a solution of the form

$$\begin{aligned} p_1 = &\sum_{n=1} e_n(\zeta) \{f_n(y) \sin 2n\pi x + g_n(y) \cos(2n-1)\pi x\} \\ &+ \sum_{n=0} o_n(\zeta) \{h_n(y) \sin(2n+1)\pi x + j_n(y) \cos 2n\pi x\} \end{aligned} \tag{3.6}$$

in which o_n is an odd function of ζ and e_n an even function and f_n, g_n, h_n and j_n are arbitrary functions of y. Investigation of (2.29) using (2.26) reveals that when $b(\tau) = 0$ a solution p_1 which has the form (3.6) initially retains it. When p_1 is given by (3.6) it contains no amplitude in an even function of ζ with sin πx dependence so from (2.41) $b_\tau = 0$ for solutions of this form. The initial conditions (2.37) - (2.39) are also of this form so $b(\tau) = 0$ and p_1 retains the symmetries of (3.6). Since the component of the source function for p_1 with cos πx dependence is an even function of ζ, the l.h.s. of (2.41) can be evaluated by doubling the contribution from the region $\zeta > 0$.

The potential vorticity of the zonal flow is zero on the critical level. Since p_1 is conservatively advected by horizontal motions it remains zero on $\zeta = 0$ for all τ (that the initial state does have $p_1 = 0$ on $\zeta = 0$ may be verified from (2.37) - (2.39)). Hence p_1 need not be calculated explicitly on $\zeta = 0$. The initial field $p_1(\tau = 0)$ and the streamfunction φ_1 (with $b(\tau) = 0$) at all times τ also have the following symmetry

$$\begin{aligned} p_1(-x + l_s/2, y, -\zeta) &= -p_1(x, y, \zeta) \ \textit{initially} \\ \varphi_1(-x + l_s/2, y, -\zeta, \tau) &= -\varphi_1(x, y, \zeta, \tau) \end{aligned} \tag{3.7}$$

Solutions of (2.29) also retain this symmetry so the potential vorticity below the steering level is related to that above by

$$p_1(-x + l_s/2, y, -\zeta, \tau) = -p_1(x, y, \zeta, \tau) \ . \tag{3.8}$$

It is desirable that the initial amplitude of the wave be chosen to ensure that p_1 has no closed contours within the critical layer initially. These form first (as γ is increased) near the sidewall. Comparison of the initial fields of P_{1y} and p'_{1y} shows that $|P_{1y}| > |p'_{1y}|$ and hence there are no closed contours when

$$\gamma |\rho_{sy}| < c_1 \ at \ y = 0, 1 \ . \tag{3.9}$$

Results

In all the experiments to be presented the zonal flow has $a_s = 0{\cdot}5$ (see (2.5)) and the channel aspect ratio $l_s = 2\pi$. For these settings the linear growth rate $c_1 \equiv 0{\cdot}175$. Each integration starts from the linear normal mode solution with an initial amplitude $\gamma{=}0{\cdot}02$ (which satisfies (3.9)) at time $\tau = 0$ and proceeds for at least 1800 steps to $\tau = 27$.

In experiment A there are 10 equally spaced levels between $\zeta = 0$ and $\zeta = 0{\cdot}35 = 2\,c_1$, their spacing DZ1 being 0·035. On each of these levels there are 128 points along the channel and 64 points across it, i.e. IXPTS = 128 and IYPTS = 64. There are 26 levels above $\zeta = 0$ in all, the highest being at $\zeta = 2{\cdot}64$. On this level IXP = 16 and IYP = 8. The domain covered extends to about $\zeta = 2{\cdot}87$ so the vertical truncation of the domain is expected to introduce a relative error of about 5% in the initial growth rate. In order to simulate the inviscid problem, biharmonic diffusion was employed with weak dissipation coefficients; $\nu_d{=}0$, $\nu_b{=}3.10^{-8}$.

The parameters detailed above for experiment A are summarised for all the experiments in table 1. The timestep used for all experiments is $\Delta\tau{=}0{\cdot}015$. This comfortably satisfies the CFL condition on all levels. Solutions were found to be insensitive to the Robert parameter R_f provided it lay between 10^{-4} and 10^{-2}. $R_f = 10^{-3}$ in all experiments presented. The experiments were performed on the CRAY Y-NP at the UK Met. Office. The most expensive occupied one of the eight CPUs for 80 seconds during which time it performed an average of about 140 Mflops.

The amplitude $a(\tau)$ of the streamfunction as a function of time in experiment A is plotted in figure 1. It reaches a first maximum near $\tau = 16$, a minimum near $\tau = 32$ and a second maximum near $\tau = 44$. Clearly the integration is too short to determine whether the flow will reach a wave-like steady state or vacillate indefinitely. Figure 2 depicts the potential vorticity field multiplied by B, Bp_1, on level $\zeta{=}0{\cdot}105$ at times $\tau = 0$, $\tau = 9$ and $\tau = 18$. The streamfunction on the same level at these times is presented in Figure 3 and Bp_1 at times $\tau = 27$, 36 and 54 in Figure 4. In the latter figure Bp_1 is clearly assuming fine structure and large gradients with sharp corners in the contours of constant Bp_1. Irreversible deformation of the p. v. contours (McIntyre and Palmer 1985) due to advection by the streamfunction is certainly occurring within non-dimensional depths of the order of $\Delta B\ c_1$ of the steering level. Figure 5 displays the solution on level $\zeta{=}0{\cdot}21$ at times $\tau = 0$, 18 and 27 where the distortion of the potential vorticity field is less intense. At the highest level in the simulation (not shown) Bp_1 is dominated by the zonal flow and the wave's perturbation to the contours barely perceptible. The qualitative nature of the solutions is discussed further at the start of the next section.

Experiments B to E were performed to investigate the sensitivity of experiment A to various parameters. Figure 6 presents the fields of Bp_1 obtained in experiments B, C and D at time $\tau = 27$ on level $\zeta{=}0{\cdot}105$ which may be compared with that for A (figure 4(a)). Table 2 provides the values of the amplitude $a(\tau)$ obtained in each experiment at times $\tau = 9$, $\tau = 18$ and $\tau = 27$.

Experiment B is a repeat of A with the diffusive parameter reduced by a factor of 10. At this setting diffusion cannot quite control the grid scale roughness which develops from corners in the Bp_1 contours (see fig. 6(a)). The amplitudes obtained in A and B nevertheless agree to within 1% for $\tau<18$ and 3% at $\tau{=}27$. In areas with strong gradients of Bp_1 the contours are noticeably tighter in experiment B than A. The lack of tightening of contours in experiment A after $\tau = 27$ (figure 4) may thus be due to the diffusion used.

Experiment C is a repeat of A except that the top four levels used in A are not present in experiment C. In C, I(h) is evaluated with h = 1·60. The ratio of the amplitudes obtained during A and C at τ=9 is comparable with the ratio of their values for I(h). Comparison of figures 6(a) and 6(b) shows that the advection is slightly further advanced in experiment C in which the wave amplitude is generally larger (for τ<27). Experiment D is a repeat of C with the horizontal resolution in each direction halved on every level. On the top level, ζ= 1·40, IXP=16 and IYP=8. The diffusive parameter is too small to control grid scale roughness fully (compare figures 6(a) and 6(c)) but the amplitudes in experiments C and D agree to within 2% for τ<18 and within 4% at τ=27. Finally experiment E is a repeat of A except that the vertical spacing between levels is doubled whilst the top of the domain is almost unaltered (h= 2·53). Differences between A and E are very slight (see table 2) and may be accounted for by the slight drop in h between A and E (c.f. with A and C).

We conclude that the qualitative form of the variation of the amplitude in figure 1 is representative of that for the inviscid problem but that the amplitude at the first maximum is probably about 5% larger than would be obtained in the inviscid case. The potential vorticity fields from run A are also fairly reliable but probably underestimate the strongest gradients when τ>18 .

A single experiment, F, is presented to illustrate the effect of moderate diffusion on the potential vorticity evolution in the critical layer. F is a repeat of A except that ν_b is set to zero and $\nu_d=3.10^{-4}$. Figure 7 displays the fields of Bp_1 obtained for experiment F on level ζ = 0·105 at times τ = 9, 18 and 27. Comparison with figure 1, which displays the corresponding fields for experiment A, shows that the distortion of the field of Bp_1 is severely limited by diffusion of this order. From table 2, it is clear that the diffusion also retards the initial growth of the wave, indeed when $\nu_d>10^{-3}$ the inviscid normal mode analysis on which the work of section 2 is based is probably inappropriate.

4. DISCUSSION

Qualitative nature of solutions

The qualitative nature of the potential vorticity fields presented in the last section is similar to that of the solutions derived by Warn & Gauthier (1989) and Warn & Warn (1978). The evolution of the complex spatial structure of the fields is perhaps most easily grasped by consideration of the advection of a segment such as AB in Figure 3b by the streamfunction shown in that figure. Note that AB follows closely an original q contour (Figure 2a). Point A is advected about a closed streamline encircling the centre of the domain whilst B is advected about the other gyre. A point close to C must be advected ever more slowly towards the stagnation point C′ of the flow. The segment connecting A and B must remain unbroken. After the fluid parcel at A has circled n times around its gyre, the advected segment must spiral (at least) n times around the gyre's centre before connecting to the parcel originally at C, which has moved close to C′.

As discussed by Rhines and Young (1983), differential rotation with angular velocity $\omega(r)$ about a closed gyre with steady streamlines results in cross-stream shearing of fields of passively advected tracers. Two fluid parcels on streamfunction contours distance Δr apart will have executed a different number of revolutions about the gyre after a time

$$\tau \simeq -\frac{T}{\omega} \omega_r \Delta r \ , \qquad (4.1)$$

where r is the average radial distance of the parcels from the centre of the gyre and T the average period of one circulation about it. After this time, the potential vorticity averaged over the distance Δr perpendicular to the flow will be an average of the initial potential vorticity around the contour. In other words, the coarse-grain potential vorticity will become streamwise homogenised.

When the streamfunction is steady, all parcel trajectories are orbits or fixed points. It is an intrinsic feature of the problem posed in this paper, however, that the structure of the streamfunction in the critical layer changes with the amplitude of the wave. If after its initial growth the amplitude of the main wave settled into an oscillation of small amplitude about a value at which the streamfunction (at a given level) had some closed gyres, some trajectories at that level could well be chaotic. This can be seen by considering a trajectory which passes close to the stagnation point C′. On returning to the vicinity of C′, depending on the time of its transit and the period of the wave it may return to one or other side of C′. The situation is somewhat similar to that of the transition to chaos via a homoclinic orbit in the Lorenz equations. Close to that transition trajectories can be constructed which execute any order of passes to the left or right of the fixed point corresponding to C′ (Sparrow 1982).

Influence of waves on zonal flow

The influence of potential vorticity homogenisation on the zonal flow can be inferred from the arguments of McIntyre & Norton (1990) concerning balanced flows which are uniquely specified by their potential vorticity field and the thermal field at their boundaries. For the quasi-geostrophic equations the streamfunction is obtained from the potential vorticity by inverting an operator (a Laplacian) which does not depend on the flow itself. Hence the effect of a wave on the zonal flow is uniquely specified by its zonal mean lateral fluxes of potential vorticity and of temperature at the boundary. There are no zonal mean thermal

fluxes for the internal baroclinic jet discussed in section 2 and at $O(\Delta B^2)$ the sole effect of the wave on the zonal flow is determined by its zonal mean lateral flux of potential vorticity, J^w, in the critical layer. McIntyre and Norton show that the zonal mean lateral p.v. flux produced by a zonally invariant force $F = A \times k$ (where k is the upward pointing unit vector) is A. Thus the effect of the wave on the zonal flow is the same as that of the "effective" force,

$$F_{eff} = J^w \times k \ , \qquad (4.2)$$

in the wave's absence.

Above the steering level, the zonal flow studied in section 2 has $U > 0$ and $Q_y > 0$. Fluxes of q tending to erode the potential vorticity gradients are hence negative and F_{eff} is in the opposite direction to the zonal flow. Below the steering level $U < 0$ and $Q_y < 0$ and the effective force is again directed so as to weaken the zonal flow.

Non-generic aspects of problem posed

Two aspects of the problem posed in section 2 are rather artificial and "non-generic". Firstly the steering level of the neutral mode is flat. Horizontal advection by the neutral mode consequently does not advect a fluid parcel out of the critical layer. When the steering level varies with the lateral ordinate a fluid parcel can be advected out of the critical layer. If the critical layer has (non-dimensional) slope of order 1 the velocity of $O(\Delta B)$ advects a parcel out of the layer in a time of O(1), and the advection within the critical layer has no time in which to act so the analysis of section 2 collapses. For this case advection within the critical layer only becomes of importance when the wave amplitude and hence the depth of the critical layer becomes comparable with the lateral variation in the depth of the steering level. This is one of several reasons presented in this section for not expecting the analysis of section 2 to hold in practice in the limit $\Delta B \rightarrow 0$.

The non-singular nature of the critical level is the second "non-generic" feature . There is no particular reason why the contours of constant Q_y should coincide precisely with isotachs of the zonal flow. Hence even if there is a contour on which $Q_y = 0$ the steering level will not usually coincide with it precisely. Neutral modes on such flows have singular values of potential vorticity at the steering level (see (1.6)). As noted in section 2 the inner equations allow room for such fields of potential vorticity which are at a higher order than those that dominated the solution of the non-singular problem. It hence seems very likely that for very small values of ΔB the evolution in the critical layer will usually be quite different from that studied in this paper.

The analysis was undertaken despite an appreciation of this point for three reasons. Firstly it seems worth elucidating the simpler problem first, making it clear that the evolution in the critical layer can be important whether the steering level is singular or not. Secondly it is not clear how to calculate appropriate singular neutral modes about which to pivot the analysis. Finally at moderate amplitudes providing the slope of the steering level is fairly small (as it is in rotating annulus experiments) the simpler analysis presented here may be more relevant than that based on singular neutral modes.

Stability of solution

Figures 4 and 6 show that strong horizontal gradients of potential vorticity develop within the critical layer. There are regions where the gradients are approximately perpendicular to the streamfunction contours and of opposite sign above and below the critical level. Killworth & McIntyre (1985) and Haynes (1989) have demonstrated that Stewartson's analytical solution for the development of a forced barotropic Rossby wave impinging on a critical layer, which develops similar reversals in potential vorticity gradients, is unstable to waves of small wavelength. It seems unlikely, however, that the solution developed in this paper is subject to similar rapid instabilities. In order to see this, note first that any solution of (2.29) excludes such instabilities because the advecting streamfunction is forced to be of the form (2.26). Linear perturbations to waves (other than the gravest mode) are conservatively advected by (2.29). Instabilities of azimuthal wavenumber k higher than that of the basic wave require a perturbation streamfunction $\delta\psi_1'$ of wavenumber k within the critical layer. If $\delta\psi_1'$ has a steady shape outside the steering level and moves with it, it will have hyperbolic dependence on z outside the critical layer

$$\begin{aligned} \psi_1' &= a\cosh\{\alpha^{(k,l)}(z-\tfrac{1}{2})\}\,\rho^{(k,l)}(y) \quad , z > 0 \\ &= a\cosh\{\alpha^{(k,l)}(z+\tfrac{1}{2})\}\rho^{(k,l)}(y) \quad , z < 0 . \end{aligned} \tag{4.3}$$

By (2.34), $\varphi_{2\zeta\zeta}$ would need to be non-zero to match the jump in ψ_{1z}' across the critical layer. As noted after (2.28), this quantity is zero within a non-singular critical layer. In other words the only normal mode with its steering level at mid-level is that of the basic wave. So the first order streamfunction in the critical layer is forced to be proportional to that of the neutral normal mode and instabilities involving other azimuthal wavenumbers are only possible in higher order solutions.

Neglect of vertical advection

The restriction of the solutions of section 2 to waves of moderate amplitude also emerges from an examination of the conditions under which the solution satisfies the quasi-geostrophic equations. The neglect of the ageostrophic horizontal velocities requires Ro << ΔB. It is plausible that no qualitative errors would arise from their neglect but as we now show the neglect of vertical velocity advection also requires Ro << B ΔB. Let

$$w = Lw^* / (U_0 H) \tag{4.4}$$

be the non-dimensional form of the vertical velocity w*. Then according to quasi-geostrophic theory

$$w \simeq -\frac{Ro}{B} D_g\psi_z / Dt \ . \tag{4.5}$$

In the critical layer

$$D_g\psi_z / Dt \simeq \Delta B \varphi_{1x}\Phi_{1y\zeta} \tag{4.6}$$

so

$$O\left(\frac{w\partial/\partial z}{u\partial/\partial x}\right) = Ro\,/\,B^2\ .\ (\Delta B\,/\,B)^{-1}\ . \qquad (4.7)$$

Vertical advection should only be neglected if Ro $<<$B^2 (ΔB / B).

Note, however, that this condition concerns the validity of the quasi-geostrophic equations. The conservation of potential vorticity in these equations is simply an analogue of the conservation of Ertel potential vorticity following parcels on isentropic surfaces. Hence (4.7) need not be viewed as a necessary condition for evolution in a critical layer to be relevant.

Effects of diffusive fluxes

Diffusive transports have been deliberately neglected (or in the numerical solutions minimised) to this point in the interest of formulating a well posed problem. A zonal flow which is laterally sheared at the horizontal boundaries will, in a viscous fluid, induce Ekman pumping of axisymmetric vertical motion which will affect the whole of the flow. The stability of such a zonal flow with its meridional circulation is a major problem in its own right.

Diffusion will, of course, play a dominant role in the critical layer (Drazin & Reid 1981 p 421) when the wave amplitude is small enough. Conditions under which advection dominates diffusion may be found by inserting the scaling used in section 2 into the diffusive version of the potential vorticity equation, which in dimensional form is

$$D_g^* q^*/Dt^* = \left(\nu^* \nabla_h^{*2} + \kappa^* f^2\,/\,N^2 \partial^2\,/\,\partial z^{*2}\right) \nabla_3^{*2} \psi^*\ . \qquad (4.8)$$

At O (ΔB^2) in the critical layer one obtains

$$\Delta B^2\, D_g Bp_1\,/\,Dt = \frac{\kappa L^2}{\Delta B H^2}\varphi_{3\zeta\zeta\zeta\zeta} + \Delta B(\kappa + \frac{\nu B L^2}{H^2})\, \nabla_h^2 \varphi_{3\zeta\zeta} + \Delta B\, \nu B\, \nabla_h^4 \varphi_1\ . \qquad (4.9)$$

where

$$\nu = \nu^*/(U_0 L) \quad and \quad \kappa = \kappa^*/(U_0 L)\ . \qquad (4.10)$$

The inviscid critical layer theory requires

$$\frac{\kappa L^2}{H^2 B^3} << (\Delta B\,/\,B)^3\ ,\ \frac{\kappa}{B} + \frac{\nu L^2}{H^2} << (\Delta B\,/\,B) \ and\ \nu << \Delta B\ . \qquad (4.11)$$

The generation of sharp gradients of Bp_1 within the critical layer makes dissipative processes important even when ΔB/ B is large enough for them to be formally small according to the above scaling arguments. Diffusive transports will control the total enstrophy within the critical layer and dissipate the strongest gradients of Bp_1. Figure 7 shows that even when (4.11) is satisfied by several orders of magnitude diffusive fluxes limit the gradients of Bp_1 as soon as the wave reaches its first maximum in amplitude.

Two-layer fluid experiments

The order of the transition in 2-layer experiments (Hart 1979) is qualitatively different from that found in thermally forced experiments (White 1988). As the inverse Froude number (the analogue of the Burger or thermal Rossby number) is decreased the 2-layer system passes from axisymmetric flow to steady waves and then to amplitude modulated waves. In the thermally forced experiments the transition is usually from axisymmetric flow to amplitude vacillations and then steady waves. Hart (1972) has investigated the lateral structure of the two-layer flows. He argues that each layer's depth independent axisymmetric zonal flow is arrested by a Stewartson type $E^{1/4}$ layer (E being the Ekman number) whilst the zonal motions of wave perturbations are halted by a viscous Stokes layer. The latter is thinner than the Stewartson layer in most experiments so that much of the axisymmetric flow's lateral shear in its side boundary layer should probably be viewed as being within the inviscid domain of the perturbation field. For a wave with a phase velocity intermediate between those of the two layers, the arguments of section 1 imply that the wave amplitude will be governed by Landau's equation which supports steady waves but not amplitude vacillations. Strongly non-linear evolution in one of the layers will only occur if the layer's zonal velocity happens to coincide with the wave's phase speed. Whilst there are particular cases in which this occurs (Pedlosky 1982b, Warn & Gauthier 1989) along most of the axisymmetric transition it does not.

5. APPLICABILITY TO ROTATING ANNULUS EXPERIMENTS

Laboratory experiments with differentially heated rotating annulus experiments are well known and have been reviewed by several authors (e.g. Read 1988 and Hide & Mason 1975). In brief, the experiments concern a fluid (typically a water-glycerol solution) contained within a concentric cylindrical annulus. The inner and outer sidewalls of the container are conductors and its base and lid are insulators. All the walls of the container are rotated together at a uniform rate Ω and a constant temperature difference ΔT is imposed between the outer and inner walls. For a given apparatus the post-transient flows which can be obtained depend chiefly on the thermal Rossby number Θ and the Taylor number Ta;

$$\Theta = g\alpha\Delta T H / (\Omega^2 L^2) \; ; \; Ta = 4\Omega^2 L^5 / (\nu^{*2} H) \; . \qquad (5.1)$$

For values of $\Theta > 2$ the flow evolves to an axisymmetric state on which only "weak" waves are found. Providing $Ta > 10^6$, on slowly decreasing Θ a sharp transition to large amplitude azimuthally varying waves is found. This transition is often referred to as the upper axisymmetric transition (UAT). The number of wave lobes at the transition is small (typically less than 3) and decreases to one as the Taylor number is increased.

These waves have long been thought to draw their energy from the available potential energy of the stably stratified baroclinic thermal field. This interpretation is supported by the fact that the location of the UAT agrees with that predicted by calculations of the stability of simple zonal flows according to quasi-geostrophic theory as well as should be expected (Hide & Mason 1975).

The velocity profile chosen for study in section 2 was motivated by cross-sections of the thermal and zonal velocity fields obtained from numerical simulations of the axisymmetric flow near the UAT such as those presented in Figure 8. The numerical model used in these simulations is described by Hignett et al. (1985). It integrates a finite difference formulation of the incompressible non-hydrostatic Navier Stokes equations discretised on a grid with enhanced resolution in the side and Ekman boundary layers.

When $a_s = 0.5$, the transitional value of the Burger number according to (2.5) is about 1.5, corresponding to a value for $\Theta = 6$. This value is well into the weak wave regime at the Taylor numbers which can be explored with greatest control in the laboratory. For the Eady profile, inclusion of Ekman pumping brings the Burger number and wavenumber at the transition to unstable normal modes into good agreement with experimental results for the UAT and it is probable that similar improvements in agreement could be made for the laterally sheared flow (although the axisymmetric vertical velocity induced by Ekman pumping raises doubts about this).

A second point relevant to the interpretation of the experiments in terms of the analysis of this paper is evident from figure 8(c) which displays

$$-\partial Q^* / \partial r^* = -\frac{1}{L^2}(1/r(rU^*)_r)_r - \frac{4\Omega^2}{\alpha g H^2 L}(U^*_z / \hat{T}_z)_z \; . \qquad (5.2)$$

Here, as elsewhere, asterisk superscripts denote dimensional variables, U^* is the zonal velocity component, and $\hat{T}$ denotes the horizontal average of T^* at a given level. $-\partial Q^* / \partial r^*$ is a dimensional formulation of the analogue of Q_y for cylindrical co-ordinates. From figure 8 it appears that in the main body of the fluid the $\partial Q^* / \partial r^* = 0$ contour follows the slope of

the isotherms and intersects the isotach U = 0 of the zonal flow quite steeply. Some caution is thus required when waves on such flows are interpreted using the analyses of waves with non-singular critical layers presented earlier.

Exact agreement between the laboratory (or numerical) experiments and the analysis presented in this paper is clearly out of the question. Rather the analysis can most usefully be taken to suggest that:

(a) strongly non-linear evolution of the potential vorticity field can be confined to a relatively narrow layer near mid-level

(b) the advection in this layer plays a crucial role in arresting initial wave growth

As a necessary preliminary to diagnostic calculations using laboratory or numerical data the following sub-section is devoted to scale analyses which seek to determe whether other conditions required for the validity of the analysis are satisfied by the parameter regimes most commonly explored in the laboratory experiments.

Scale analyses

In these calculations we take

$$L = 5\,cm\ ,\ H = 15\,cm,\ l_s = 2\pi\ ,\ \varrho = 1\,g\,cm^{-3}$$
$$\nu^* = 1{\cdot}6.10^{-2}\,cm^2\,s^{-1}\ ,\ \kappa^* = 1{\cdot}3.10^{-3}\,cm^2\,s^{-1}\ . \qquad (5.3)$$

Calculations will be performed explicitly for waves at two points in parameter space :

$$\text{Case(a): } \Delta T = 4\,K\ ,\ \Omega = 0{\cdot}5\,rad\,s^{-1}\ ;\ U_0 \simeq 0{\cdot}5\,cm\,s^{-1}\ ,\ \Theta \simeq 2 \qquad (5.4a)$$

which is close to the UAT (see figure 8) and

$$\text{Case(b): } \Delta T = 4\,K\ ,\ \Omega = 1{\cdot}0\,rad\,s^{-1}\ ;\ U_0 \simeq 0{\cdot}2\,cm\,s^{-1}\ ,\ \Theta \simeq 0{\cdot}5 \qquad (5.4b)$$

which is in the middle of the regular wave regime and at a point explored in some detail by Hignett et al. (1985). We assume that the number of lobes, n, in the developing wave is 2 in case (a) and that n=3 in case (b).

(i) Diffusive fluxes

Conditions for the diffusive fluxes within the critical layer to be formally small are provided by (4.11). Substituting the values defined in (5.3) and (5.4) yields the requirements that

$$case(a)\ (\Delta B/B)^3 >> 5.10^{-4}\ ;\ \Delta B/B >> 10^{-2} \qquad (5.5a)$$

$$case(b)\ (\Delta B/B)^3 >> 7.10^{-2}\ ;\ \Delta B/B >> 10^{-1}\ . \qquad (5.5b)$$

When $\Delta B/B = 0.2$ conditions (a) are fairly well satisfied, the right hand terms being 20 or more times smaller than those on the right. The first of conditions (b) is not satisfied, however, until $\Delta B/B$ is of order 1. When $\Delta B/B$ does not satisfy (4.11) it may be more appropriate to consider a diffusive critical layer than an advective one.

Comparison of (3.1) and (4.9) suggests that the most appropriate expression for ν_d to use

for comparison with laboratory experiments is

$$\nu_d = (\kappa / B + \nu L^2 / H^2)(B / \Delta B) . \qquad (5.6)$$

Using (5.1), (5. 3) and (5.4) again one finds that

$$case\,(a)\,\nu_d \simeq 2.10^{-3} / (\Delta B / B) \; ; \; case\,(b)\,\nu_d \simeq 10^{-2} / (\Delta B / B) . \qquad (5.7)$$

The simulation with ν_d as small as $2 . 10^{-4}$ had a marked effect on the evolution of Bp_1, limiting the tightening of contours, so we conclude that diffusive influences severely limit the evolution within the critical layer in the annulus experiments.

Increasing the Prandtl number of the fluid and/or the aspect ratio will tend to reduce this influence of diffusion in the critical layer, increasing the range of values of ΔB/B over which (4.11) holds and reducing the effective value of ν_d in this region. Jonas (1981) reports that the fraction of the (Θ, Ta) regime diagram occupied by amplitude vacillating flows increases with the Prandtl number. Johnson (private communication) has found amplitude vacillation to become more widespread as the aspect ratio (H/ L) is increased. These results are consistent with those of Pfeffer et al. (1980) for fluids with Prandtl numbers of 21 and 73.

(ii) Growth rates and doubling periods

At small supercriticalities, the initial growth rate of the wave is slow. Indeed as the UAT is approached amplitude vacillating waves with periods as long as 600 seconds have been observed. The initial non-dimensional growth rate $k\,c_i$ of a wave is related to ΔB/B by (2.39) and (2.40),

$$kc_i = \pi n F \frac{\Delta B}{2B} , \qquad (5.8)$$

where F is a factor whose value is close enough to 1 for our purposes. The dimensional time τ_d required for the wave to double in amplitude is hence

$$\tau_d = \frac{\ln 2}{kc_i} \cdot \frac{L}{U_0} \simeq \frac{1{\cdot}4}{n(\Delta B/B)} \frac{L}{U_0} . \qquad (5.9)$$

Substituting (5.2) and (5.3) in these formulae

$$case\,(a)\,\tau_d \simeq 7 / (\Delta B / B)\,s \; ; \; case\,(b)\,\tau_d \simeq 12 / (\Delta B / B)\,s . \qquad (5.10)$$

The wave vacillation presented in figure 4 of Hignett (1985), which is close to (b) in parameter space, appears to have a doubling period of about 65 seconds during its growth phase, which corresponds according to (5.10) to a value of ΔB/B = 0·2. Near the UAT, doubling periods of 65 seconds would correspond to ΔB/B = 0·1.

(iii) Vertical advection and advection out of the critical layer

For vertical advection in the critical layer to be negligible, condition (4.7) must hold. Evaluating this expression for cases (a) and (b) as before yields

$$case\,(a)\;\Delta B / B >> 0.2 \; ; \; case\,(b)\,\Delta B / B >> 1.3 . \qquad (5.11)$$

Hence neglect of vertical advection does not appear to be a good approximation in the ex-

periments at small supercriticalities. As noted in section 4, however, this condition concerns the validity of the quasi-geostrophic equations and need not be viewed as a necessary condition for evolution in a critical layer to be relevant.

The zonal mean vertical motion forced by the Ekman pumping accompanying a laterally sheared zonal flow is given by

$$|w^*| = \tfrac{1}{2}\left(\frac{2\nu^*}{f}\right)^{\frac{1}{2}} |U^*_{y^*}| \ . \tag{5.12}$$

Fluid parcels are hence advected out of a critical layer of depth $\Delta B\, H$ in a time

$$t_E = \frac{\Delta BHL}{U(\nu^*/2f)^{\frac{1}{2}}} \ ; \tag{5.13}$$

$$case\ (a)\ t_E \simeq 800\,\Delta B/B\ s \ ;\ case\ (b)\ t_E \simeq 400\,\Delta B/B\ s \ . \tag{5.14}$$

This is longer than the doubling period when $\Delta B/B > 0{\cdot}2$.

Figure 8 shows that the level at which the zonal velocity vanishes, which is close to the steering level (wave drift periods being slow) is fairly flat. Hence provided $\Delta B/B > 0{\cdot}1$ horizontal advection out of the critical layer should not disrupt the mechanism severely.

(iv) Conclusions

In summary, the critical layer evolution presented in sections 2 is more likely to be relevant near the UAT than at smaller Burger numbers. This is not simply because at lower Burger numbers several wavenumbers are unstable and hence competing for dominance but because the scaling requirements, particularly those relating to diffusive fluxes, are more likely to be satisfied there. Vacillations near the UAT in which the wave at small amplitude has a doubling time of about 50 seconds appear to be the most promising candidates.

Diagnostics

Some ingenuity might be needed to detect the presence of critical layer developments in the laboratory. The velocity acquisition system used by Dr. Hide's group is restricted to observations of the flow at a few fixed, evenly spaced levels and the thermocouple ring is standardly employed at a fixed level near mid-height. At moderate super-criticalities $\Delta B/B > 0.3$, the critical layer should cover one-third of the depth of the fluid and hence not be too elusive. Distortions of the thermal and velocity fields will however be only of $O(\Delta B/B)^2$.

Diagnostics of the potential vorticity field from integrations of the Navier-Stokes numerical model are more easily obtained. Figures 9 and 10 present such diagnostics for the two lobe (n=2) amplitude vacillating flow close to the UAT reported by Hignett et al. (1985). Figure 9 presents evaluations at 100 second intervals of the (quasi-geostrophic) potential vorticity field on the model level nearest the steering level. The vacillation period of 600 seconds is longer than that suggested above to be most suitable for comparison with the inviscid analysis, but non-linear advection of the potential vorticity field is clearly apparent in the asymmetrical and curled contours of figure 9. Figure 10, which presents streamfunction fields on the same level and p. v. fields near the base of the annulus, shows that the p. v. field away from the steering level has a less rich harmonic structure.

Only 16 vertical levels were used in the above numerical experiment. Since the vertical grid of the model is deliberately stretched to resolve the horizontal and side boundary layers the vertical resolution near mid-level is poor. Even at moderate supercriticalities it would be desirable to use 32 or 64 points in the vertical to obtain a good resolution in the neighbourhood of the steering level. The region in parameter space over which the model supports amplitude vacillation is believed to be smaller than that observed experimentally. This may well be because of the model's poor vertical resolution near mid-level.

6. CONCLUDING REMARKS

The growth of weakly unstable inviscid waves on laterally sheared baroclinic zonal flows has been argued (in section 1) to be arrested by the self-advection of their p. v. fields within "critical" layers centred on the waves' steering levels. Waves growing on flows with uniform p.v. gradients and inviscid waves on laterally uniform flows are arrested by other, weaker, non-linear interactions. Most "naturally" occurring baroclinic zonal flows will have substantial lateral shears. We contend that wave disturbances to them will be mainly controlled by the self advection within their critical layers.

A comparatively simple case in which the critical layer is non-singular has been studied in some detail (sections 2 and 3). The self-advection severely distorts the original p. v. structure within the critical layer generating some large p. v. gradients. These gradients make local diffusive fluxes much stronger than standard scale analysis would suggest.

P. v. diagnostics from a numerical simulation of an amplitude vacillating flow near the UAT (figures 9 and 10) show that as the wave grows its p. v. field is significantly distorted near mid-level. We suggest that the growth phase may be characterised by almost inviscid non-linear advection of p. v. within the wave's critical layer. During the wave's decay phase diffusive fluxes are probably important in eroding sharp p. v. gradients in the critical layer and re-establishing the axisymmetric flow. Further diagnostics of the roles of advection and dissipation in the critical layer in both laboratory and numerical experiments are needed to establish whether these suggestions are substantially correct.

An early version of this paper formed part of the author's Ph. D. thesis undertaken through the Public Research Institute Scheme at Imperial College, London and the U. K. Meteorological Office. It is a pleasure to thank R. Hide, P. L. Read and A. A. White for their advice, encouragement and assistance.

APPENDIX A. DERIVATION OF MATCHING CONDITION (2.19)

This appendix shows that the condition for equations (2.17) - (2.19) to have solutions may be expressed as (2.20).

(2.17) - (2.19) are

$$M_0\psi_{2x} = -B_0 / U\, \nabla_h^2 \psi_{1\tau} - J(\psi_1, B_0 \nabla_h^2 \psi_1) / U + U_{zz}\psi_{1x} / (B_0 U)$$

$$\psi_{2zx} = 0 \ \ on\, z = \pm ½ \qquad \text{(A.1)}$$

$$\left[\psi_2\right]_{0^-}^{0^+} = H(x,y) \ ; \ \left[\psi_{2z}\right]_{0^-}^{0^+} = I(x,y) \ .$$

The operator M_0 in the first equation above is defined by (2.15) and may be written as

$$M_0 = M_1 + \partial^2/\partial z^2 \ ; \ M_1 \equiv B_0 \nabla_h^2 + (BQ_y / U)_{B=B_0} \ . \qquad \text{(A.2)}$$

M_1 includes only horizontal derivatives and for the flow (2.5) is independent of depth (see (2.6)). Solutions of (A.1) can hence be expressed as a summation of the eigenfunctions $\rho^{(k,l)}(y)\exp(irk\pi x)$ of M_1 :

$$\psi_2 = \sum_{k,l} \psi_2^{(k,l)}(z)\, \rho^{(k,l)}(y)\, \exp(irk\pi x) \ . \qquad \text{(A.3)}$$

Projection onto the eigenfunctions of M_1 reduces (A.1) to equations of the form

$$\psi_{2zz}^{(k,l)} + \alpha^{(k,l)}\psi_2^{(k,l)} = f^{(k,l)}(z)$$

$$\left[\psi_2^{(k,l)}\right]_{0^-}^{0^+} = H^{(k,l)} \ , \ \left[\psi_{2z}^{(k,l)}\right]_{0^-}^{0^+} = I^{(k,l)} \qquad \text{(A.4)}$$

$$\psi_{2z}^{(k,l)} = 0 \ \ at\ z = \pm ½$$

in which $\alpha^{(k,l)} > 0$ for all modes other than the neutral mode, ρ_s , for which $\alpha^{(k,l)} = 0$.

When $\alpha^{(k,l)} > 0$ the complementary solutions enable solutions to be found for any $f^{(k,l)}(z)$, $H^{k,l}$ and $I^{(k,l)}$. So it is adequate to consider only the projection into $\rho_s(y)\exp(ir\pi x)$ to find the condition for (A.1) to have a solution. This projection results in a problem of the form

$$\chi_{zz} = E / \sin\pi z \ + \ F$$

$$[\chi]_{0^-}^{0^+} = R \ , \ [\chi_z]_{0^-}^{0^+} = S \qquad \text{(A.5)}$$

$$\chi_z = 0 \ \ at\, z = \pm ½$$

in which χ and F are given by

$$\chi = \iint \rho_s(y) exp(ir\pi x) \psi_{2x} \, dxdy$$
$$F = -\pi^2 / B_0 \iint \rho_s(y) exp(ir\pi x) \psi_{1x} \, dxdy \; . \tag{A.6}$$

(Explicit formulae for E, R and S are not needed below.) Integrating (A.5) once yields

$$\chi_z = E/\pi \{ \ln | \tan \pi z/2 | - \ln | \tan \pi/4 | \} + F(z - \tfrac{1}{2}) \quad , \; z > 0$$
$$\chi_z = E/\pi \{ \ln | \tan \pi z/2 | - \ln | \tan \pi/4 | \} + F(z + \tfrac{1}{2}) \quad , \; z < 0 \tag{A.7}$$

and hence

$$[\chi_z]_{-z}^{z} = F(2z - 1) \rightarrow -F \; as \; z \downarrow 0 \, . \tag{A.8}$$

This condition on the jump in potential temperature across the critical layer provides a relationship between the inner and outer solutions which must be satisfied if the solution sought is to be valid. It is the only consistency condition at this order because the complementary solution χ = const. can accommodate any jump R in the streamfunction. (2.20) is easily obtained by substituting (A.6) into (A.8).

APPENDIX B. INITIAL CONDITIONS

This appendix finds an expression for the linearly unstable normal mode in the critical layer, which serves as the initial condition for the numerical simulations of section 3.

We start by linearising (2.1) about the zonal flow (2.5),

$$q'_t + U q'_x + Q_y \psi'_x = 0 \tag{B.1}$$

and letting $B = B_0 - \Delta B$ and

$$\psi' = Re\{\phi(y,z) \, exp ir\pi(x - ct)\} \; . \tag{B.2}$$

Posing an expansion for ϕ and c in powers of ΔB

$$\phi = \Delta B \, \rho_s(y) + \Delta B^2 \, \phi_1 + \ldots \; ; \; c = \Delta B \, c_1 + \ldots \tag{B.3}$$

based on the neutral normal mode ρ_s,

$$(d^2/dy^2 - r^2\pi^2)\rho_s + (Q_y / U)\rho_s = 0 \; , \; \rho_s = 0 \; at \; y = 0, 1 \, , \tag{B.4}$$

at O(ΔB^2) one finds that

$$(B_0 \nabla_h^2 + \partial^2 / \partial z^2 + B_0 Q_y / U)\,\phi_1 = -\frac{\pi^2}{B_0}\rho_s - B_0 c_1 \frac{(Q_y/U)\,\rho_s}{U-c}$$

$$\phi_{1z} = 0 \text{ on } z = \pm ½ \,;\; \phi_1 = 0 \text{ on } y = 0,\ 1\,. \tag{B.5}$$

The Fredholm condition for (B.5) to have a solution is that the free (complementary) solution ρ_s be orthogonal to the forcing of ϕ_1. This condition determines the dependence of c_1 on ΔB. Standard manipulations show that c_1 is pure imaginary and that

$$\int\!\!\int \rho_s^2 \pi^2 / B_0 \, dy\, dz = -\int\!\!\int c_1 \frac{B_0 (Q_y/U)\rho_s^2}{U-c}\, dy\, dz = \pi\,|c_1| \int_y \frac{B_0 (Q_y/U)\rho_s^2}{|U_z|_{z=0}}\, dy\,. \tag{B.6}$$

So

$$c_1 = \frac{iT}{2B_0^2}\;;\; T = \frac{\int \pi^2 \rho_s^2\, dy}{\int \rho_s^2 (Q_y/U)(1 - a_s + a_s \sin \pi y)^{-1}\, dy}\,. \tag{B.7}$$

The ratio $T = B_0$ when $a_s = 0$ and is not far from 1 for a_s near 0.5.

Manipulation of (2.29) using (2.30), (2.26), (2.6) and (2.8) shows that $\varphi'_{3\zeta\zeta}$ for this normal mode satisfies

$$(U - c)\,\varphi_{3\zeta\zeta x} = B_0 (Q_y / U)\,\varphi'_{1\tau}\,. \tag{B.8}$$

So the normal mode with an initial outer streamfunction of small amplitude γ

$$\varphi'_1 = \gamma \cos(r\pi x)\,\rho_s(y) \tag{B.9}$$

has accompanying vertical variation

$$\varphi'_{3\zeta\zeta} = \frac{\gamma B_0 (Q_y/U)\rho_s}{|\tilde{U} - c|^2}\{\,|c|^2 \cos(r\pi x) + \tilde{U}\,|c|\,\sin(r\pi x)\} \tag{B.10}$$

in which

$$c = \Delta B c_1 \;;\; \tilde{U} = \frac{\Delta B \pi \zeta}{2}(\,1 - a_s + a_s \sin \pi y\,)\,. \tag{B.11}$$

Equations (2.37) to (2.40) are simply re-statements of (B.7) and (B.9) to (B.11).

REFERENCES

Bell, M. J., and A. A. White, 1988: The stability of internal baroclinic jets: some analytical results. J. Atmos. Sci., 45, 2571-2590.

Bell, M. J., 1989: Theoretical investigations prompted by experiments with baroclinic fluids. Ph. D. thesis, University of London, 215 pp.

Charney, J. G., 1947: The dynamics of long waves in a baroclinic westerly current. J. Meteor., 4, 135-162.

Charney, J. G., and M. E. Stern, 1962: On the stability of internal baroclinic jets in a rotating atmosphere. J. Atmos. Sci., 19, 159-172.

Drazin, P. G., 1970: Non-linear baroclinic instability of a continuous zonal flow. Quart. J. Roy. Meteor. Soc., 96, 667-676.

Drazin, P. G., 1972: Nonlinear baroclinic instability of a continuous zonal flow of viscous fluid. J. Fluid Mech., 55, 577-587.

Drazin, P. G, and W. H. Reid, 1981: Hydrodynamic stability. London, C. U. P, 525 pp.

Eady, E. T., 1949: Long waves and cyclone waves. Tellus, 1, 33-52.

Haltiner, G. J., and R. T. Williams, 1980: Numerical prediction and dynamic meteorology. New York, Wiley, 477 pp.

Hart, J. E., 1972: A laboratory study of baroclinic instability. Geophys. Fluid Dyn., 3, 181-209.

Hart, J. E., 1979: Finite amplitude baroclinic instability. Ann. Rev. Fluid Mech., 11, 147-172.

Haynes, P. H., 1989: The effect of barotropic instability on the nonlinear evolution of a Rossby wave critical layer. J. Fluid Mech., 207, 231-266.

Hide R., and P. J. Mason, 1975: Sloping convection in a rotating fluid: a review. Advances in Phys, 24, 47-100.

Hignett, P., 1985: Characteristics of amplitude vacillation in a differentially heated rotating annulus. Geophys. Astrophys. Fluid Dyn., 31, 247-281.

Hignett, P., A. A. White, R. D. Carter, W. D. N. Jackson and R. M. Small, 1985: A comparison of laboratory measurements and numerical simulations of baroclinic wave flows in a rotating cylindrical annulus. Quart. J. Roy. Meteor. Soc., 111, 131-154.

Hoskins, B. J., and A. J. Simmons, 1975: A multi-layer spectral model and the semi-implicit method. Quart. J. Roy. Meteor. Soc., 101, 637-655.

Jonas, P. R., 1981: Some effects of boundary conditions and fluid properties on vacillation in thermally driven rotating flow in an annulus. Geophys. Astrophys. Fluid Dyn., 18, 1-23.

Killworth, P. D., and M. E. McIntyre, 1985: Do Rossby-wave critical layers absorb, reflect, or over-reflect? J. Fluid Mech., 161, 449-492.

Kreyszig, E., 1982: Advanced Engineering Mathematics. New York, Wiley, 939 pp.

McIntyre, M. E., and W. A. Norton 1990: Dissipative wave-mean interactions and the transport of vorticity or potential vorticity. J. Fluid Mech., 212, 403-435.

McIntyre M. E., and T. N. Palmer, 1985: A note on the general concept of wave breaking for Rossby and gravity waves. Pure Appl. Geophys., 123, 964-975.

Pedlosky, J., 1964: The stability of currents in the atmosphere and the oceans. Part I. J. Atmos. Sci., 27, 201-219.

Pedlosky, J., 1970: Finite amplitude baroclinic waves. J. Atmos. Sci., 27, 178-200.

Pedlosky, J., 1982a: Geophysical Fluid Dynamics. New York, Springer Verlag, 624 pp.

Pedlosky, J., 1982b: A simple model for nonlinear critical layers in an unstable baroclinic wave. J. Atmos. Sci., 39, 2119-2127.

Pfeffer, R. L., G. Buzyna and R. Kung, 1980: Relationships among eddy fluxes of heat, eddy temperature variances and basic state temperature parameters in thermally driven rotating fluids. J. Atmos. Sci., 37, 2577 - 2599.

Read, P. L., 1988: The dynamics of rotating fluids: the 'philosophy' of laboratory experiments and studies of the atmospheric general circulation. Met. Mag., 117, 35-45.

Rhines, P. B., and W. R. Young, 1983: How rapidly is a passive scalar homogenized within closed streamlines? J. Fluid Mech., 133, 135-148.

Sparrow, C., 1982: The Lorenz Equations, New York, Springer-Verlag, 269 pp.

Stewartson, K., 1978: The evolution of the critical layer of a Rossby wave. Geophys. Astrophys. Fluid Dyn., 9, 185-200.

Warn, T. and P. Gauthier, 1989: Potential vorticity mixing by marginally unstable baroclinic disturbances. Tellus, 41A, 115-131.

Warn, T. and H. Warn, 1978: The evolution of a nonlinear critical layer. Studies in Applied Maths., 59, 37-71.

White, A. A., 1988: The dynamics of rotating fluids: numerical modelling of annulus flows. Meteor. Mag., 117, 54-63.

FIGURE CAPTIONS

Figure 1

The evolution of the amplitude, a, of the wave (2.16) as a function of the slow time $\tau = \Delta B\ t$ during experiment A.

Figure 2

Contour plots of the highest order potential vorticity field Bp_1 (defined by (2.30)) on level ζ=0.105 within the critical layer obtained during experiment A at slow times (a) τ=0, (b) τ=9, (c) τ=18. The contour interval is 0·2 and negative contours are dashed.

Figure 3

Contour plots as in figure 2 but for the streamfunction with a contour interval of 0·02.

Figure 4

Contour plots of potential vorticity as in figure 2 at times (a) τ=27, (b) τ=36, (c) τ=54.

Figure 5

Contour plots of potential vorticity as in figure 2 but for level ζ=0·21 with a contour interval of 0.5.

Figure 6

Contour plots of Bp_1 at time τ=27 and level ζ=0·105 obtained during (a) experiment B (b) experiment C (c) experiment D. The corresponding plot for experiment A is Figure 4a.

Figure 7

Contour plots of Bp_1 on level ζ=0·105 obtained during experiment F (in which $\nu_d = 2.\ 10^{-4}$) at times (a) τ=9, (b) τ=18, (c) τ=27.

Figure 8

Height (z) / radius (r) cross-sections of (a) the temperature (^{o}C) (b) the zonal velocity (mm s^{-1}) and (c) the lateral p. v. gradient ($-\ \partial Q^{*} / \partial r^{*}$ $cm^{-1}\ s^{-1}$) of a steady axisymmetric flow. The fields are taken from a numerical simulation using the Navier-Stokes model described by Hignett et al. (1985) with 32 (radial) x 32 (vertical) points. The inner and outer radii and depth of the annulus are 2·5, 8·0 and 14·0 cm respectively and the imposed conditions, Θ=2·17 and Ta=1·13 10^{6}, were obtained by setting ΔT=4·02 ^{o}C and Ω=0·499 rad s^{-1}.

Figure 9

Horizontal cross-sections at 100 second intervals of q^{*}, the quasi-geostrophic potential vorticity field, on model level 8 which is 5·77 cm above the base. The contour interval is 0·1 s^{-1} and negative contours are dashed. The annular geometry is as in figure 8 and the model had 64 (azimuthal) x 32 (radial) x 32 (vertical) points. The imposed conditions Θ=1·76 and Ta=2·05 10^{6}, were obtained using ΔT=4·00 ^{o}C and Ω=0·51 rad/s.

Figure 10

Figures (a), (b) and (c) re-display q^{*} at 5·77 cm above the base as presented in figures 9 (g), (h) and (i) respectively. Figures (d), (e) and (f) present the pressure at the same level and (g), (h) and (i) q^{*} at 2·00 cm above the base (model level 6) for the corresponding times. The contour interval is $5\ .\ 10^{-3}$ N m^{-2} in (d), $2\ .\ 10^{-3}$ N m^{-2} in (e) and (f) and 0·2 s^{-1} in (g) - (i). Negative contours are again dashed.

TABLE 1

The parameter settings used in the numerical experiments described in section 3.

	A	B	C	D	E	F
IXPTS	128	128	128	64	128	128
IYPTS	64	64	64	32	64	64
IZPTS	26	26	22	22	13	26
DZ1	0.035	0·035	0·035	0·035	0·07	0·035
top level	2·64	2·64	1·4	1·4	2·19	2·64
ν_b	$3\ 10^{-8}$	$3\ 10^{-9}$	$3\ 10^{-8}$	$3\ 10^{-8}$	$3\ 10^{-8}$	0.0
ν_d	0·0	0·0	0·0	0·0	0·0	$2\ 10^{-4}$

TABLE 2

The amplitude of the wave, $a(\tau)$, obtained at three times in each of experiments A - F.

$a(\tau)$	τ=9	τ=18	τ=27
A	0·0905	0·1687	0·0924
B	0·0901	0·1692	0·0956
C	0·0943	0·1739	0·0939
D	0·0922	0·1750	0·0977
E	0·0908	0·1693	0·0925
F	0·0778	0·1238	0·051

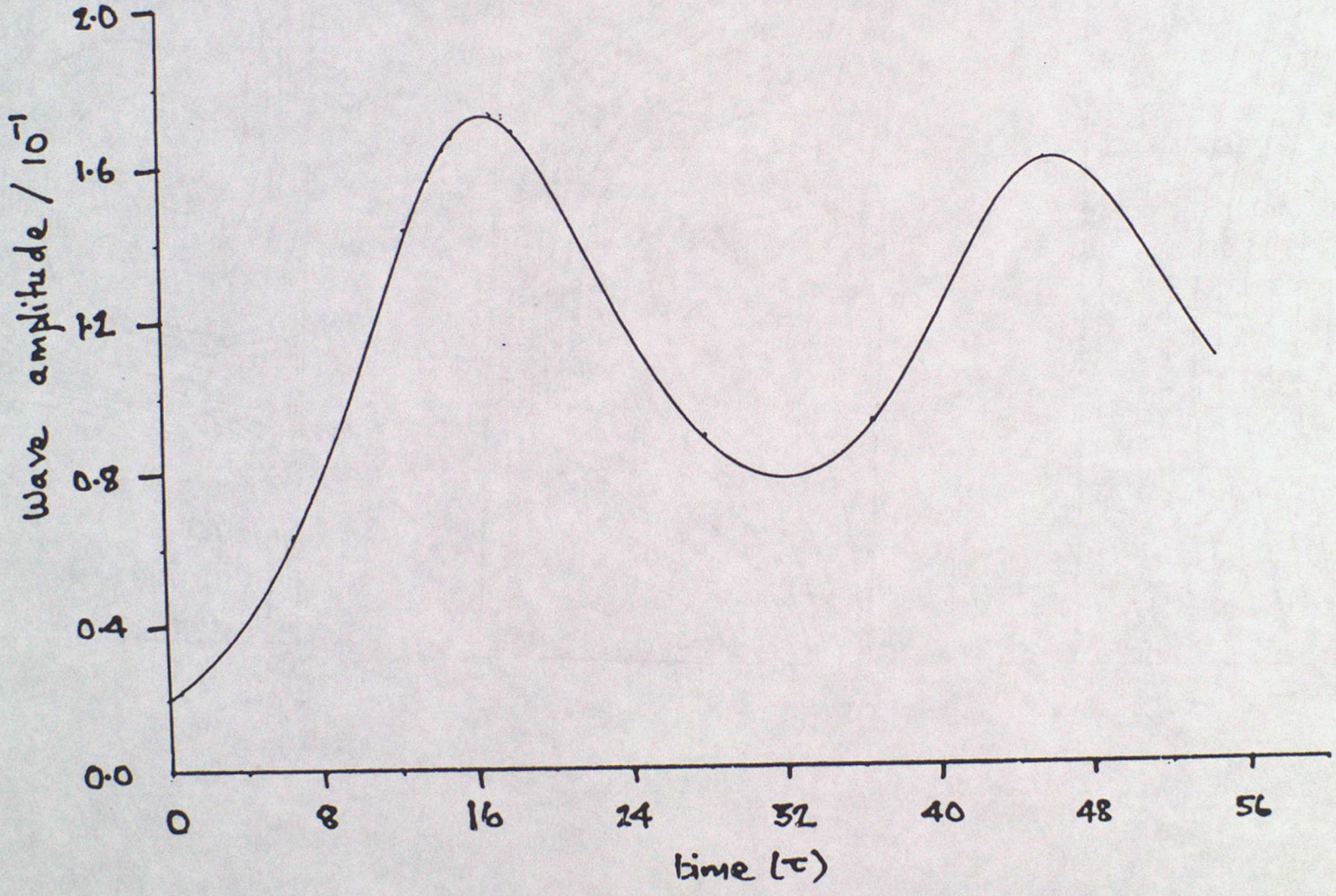

Figure 1

Figure 2

a

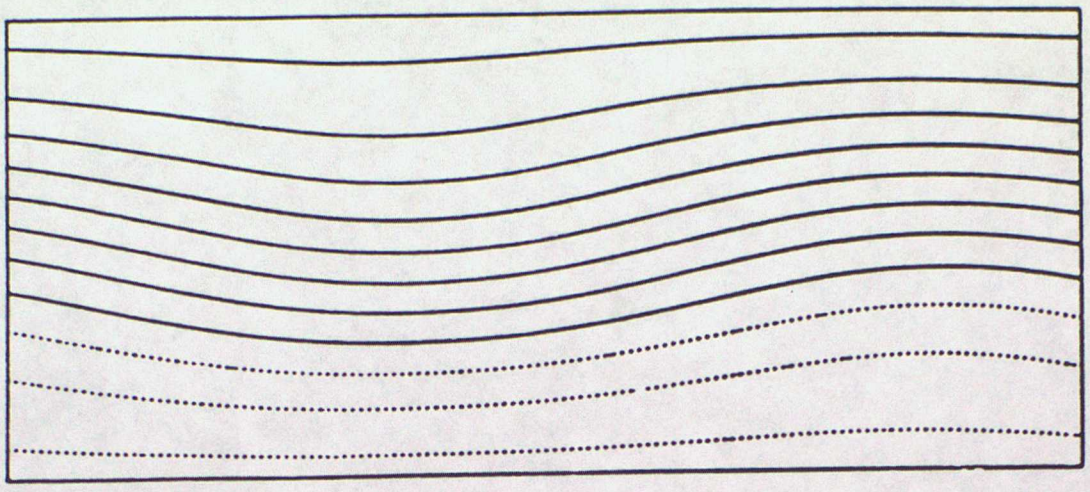

b

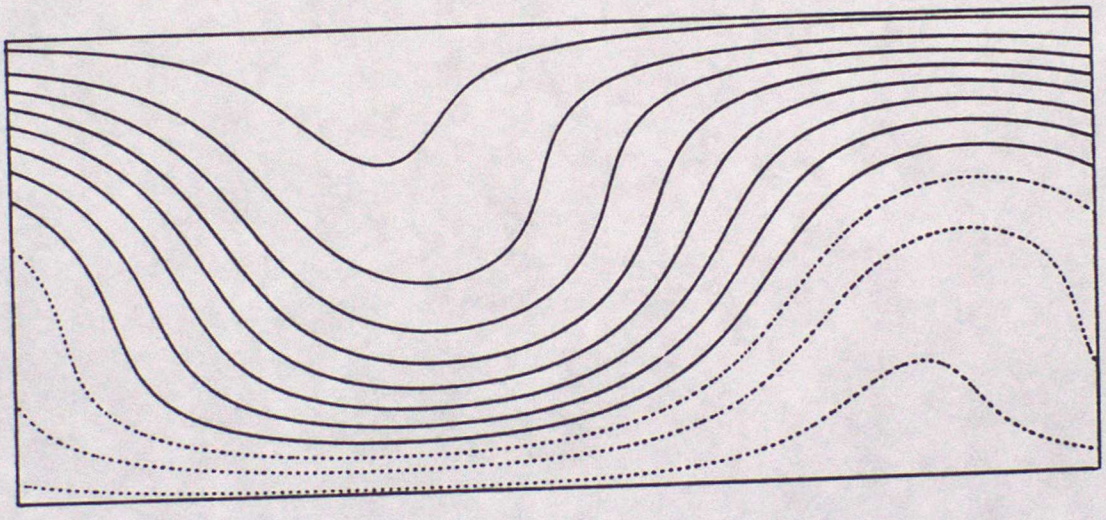

c

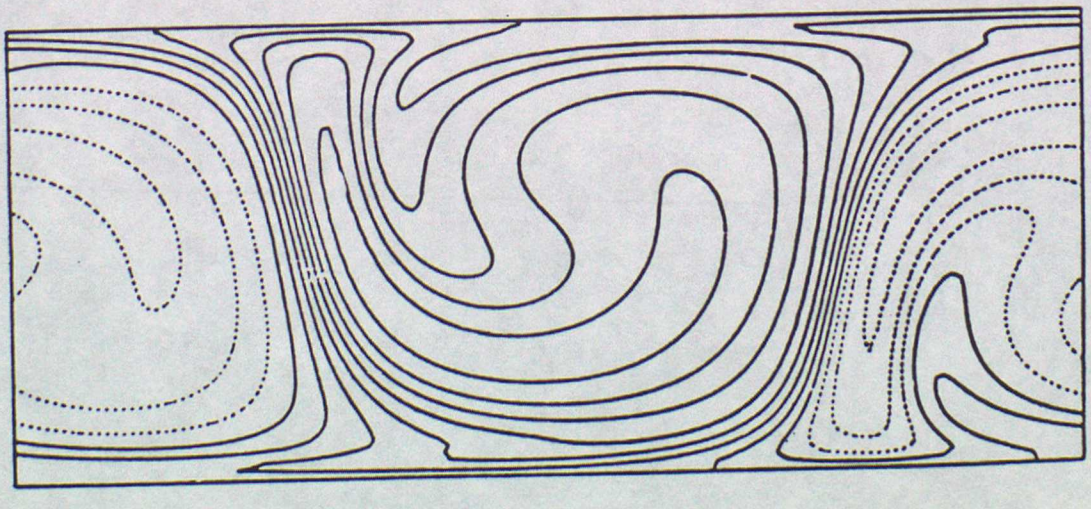

Figure 3

a

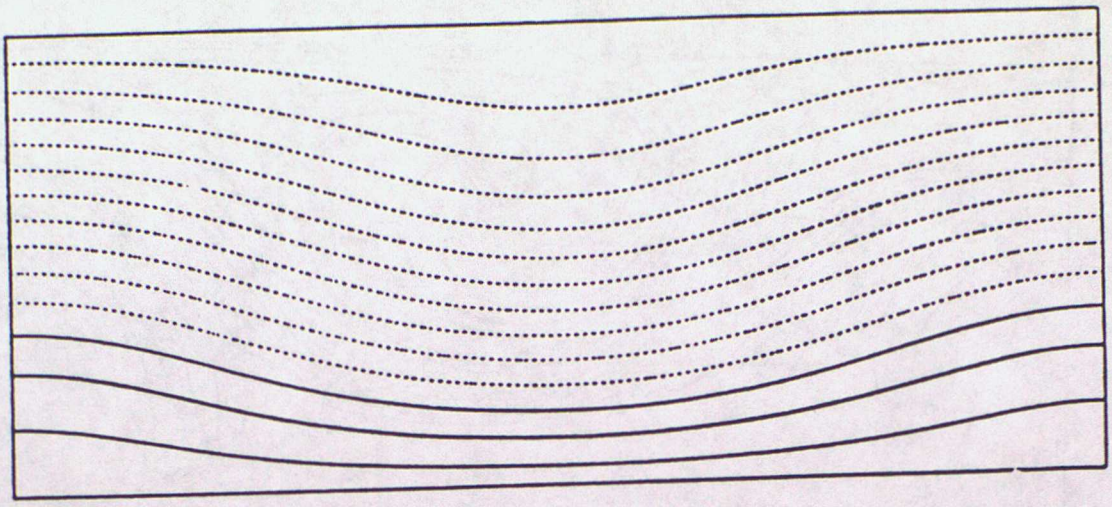

b

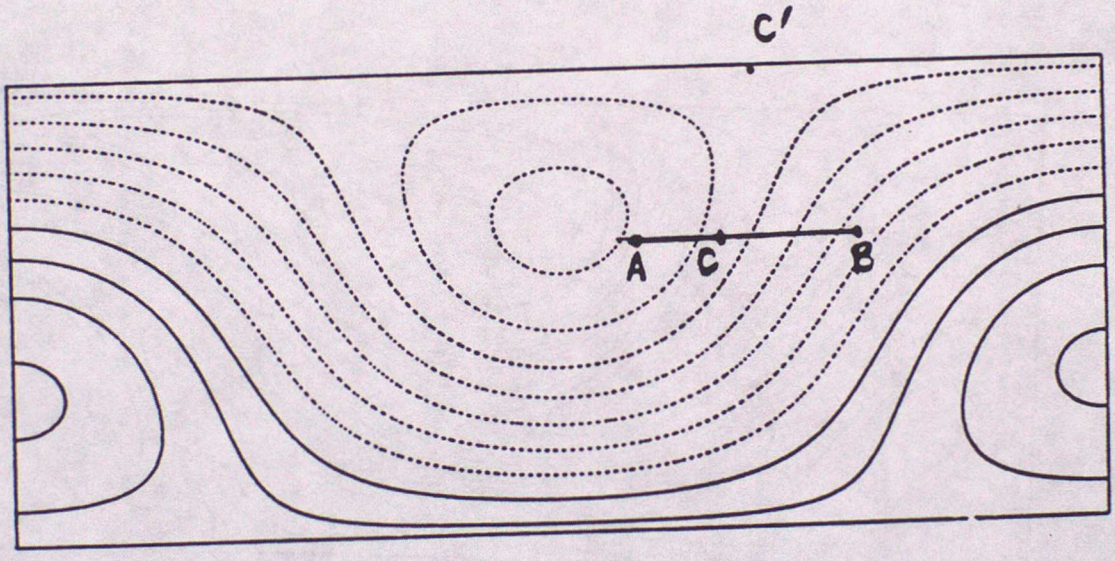

c

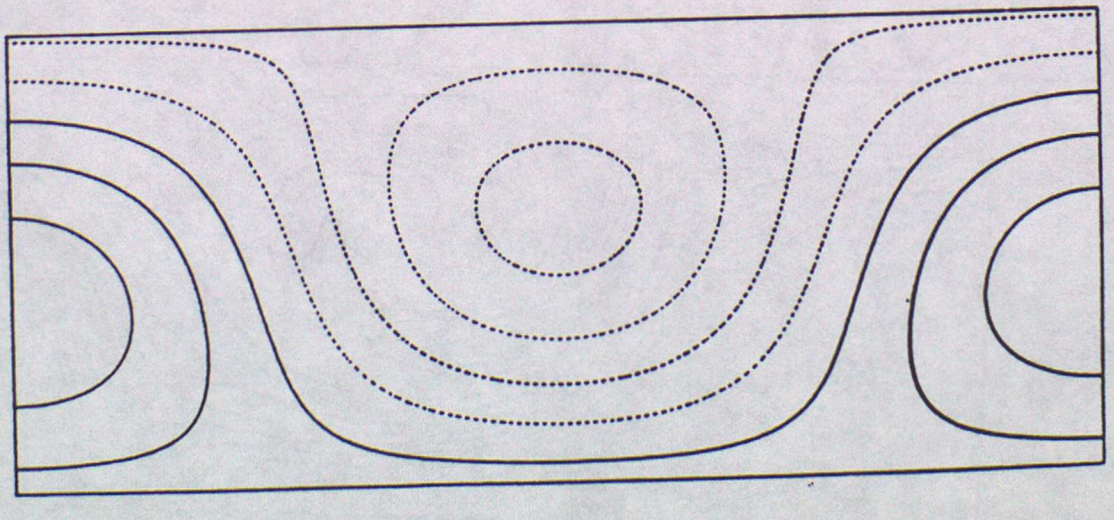

Figure 4

a

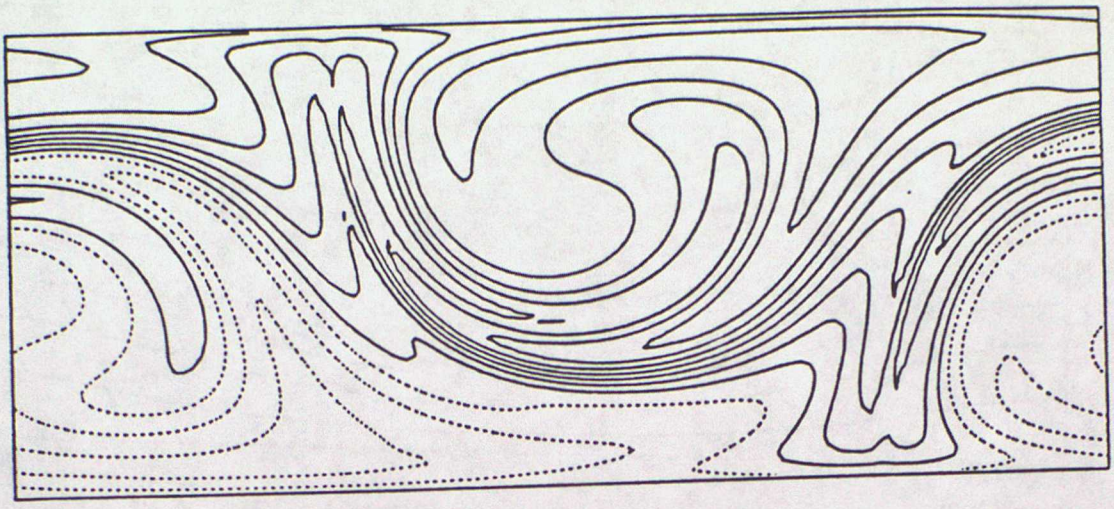

b

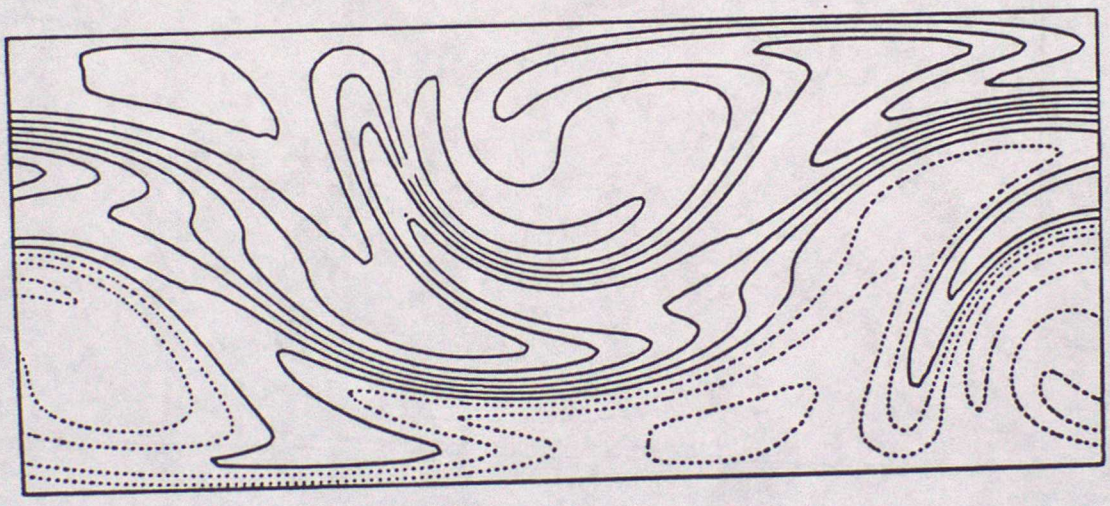

c

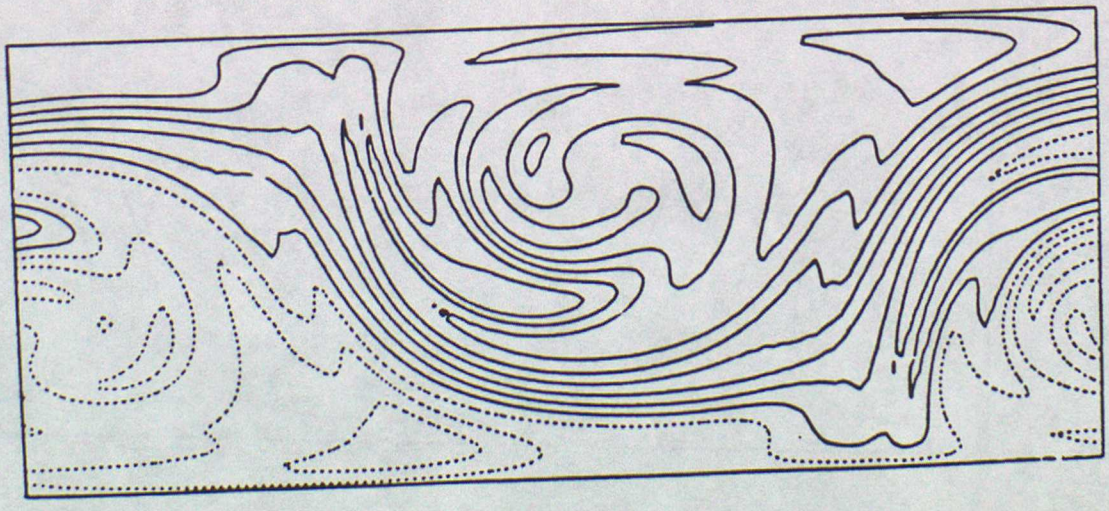

Figure 5

a

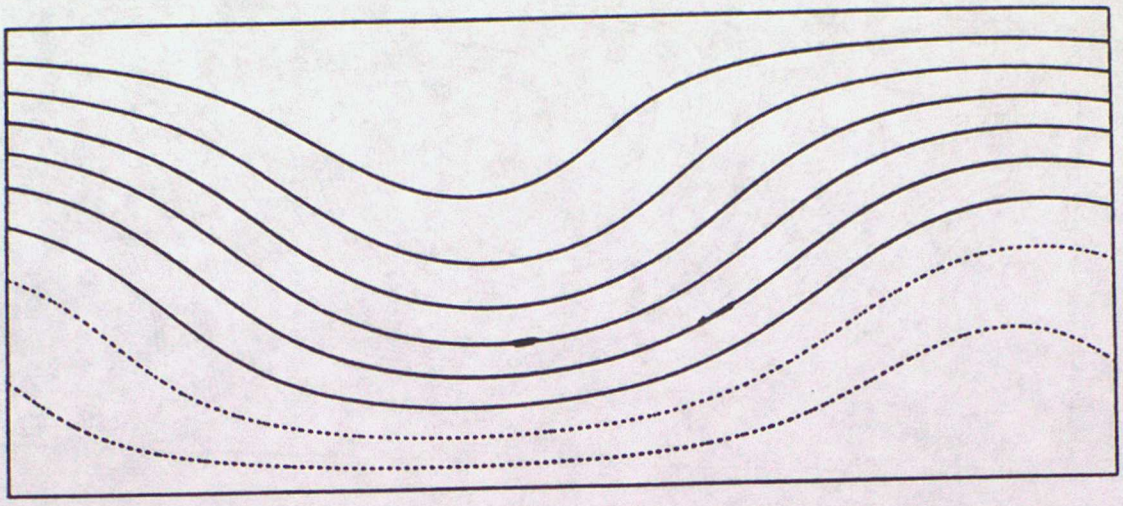

b

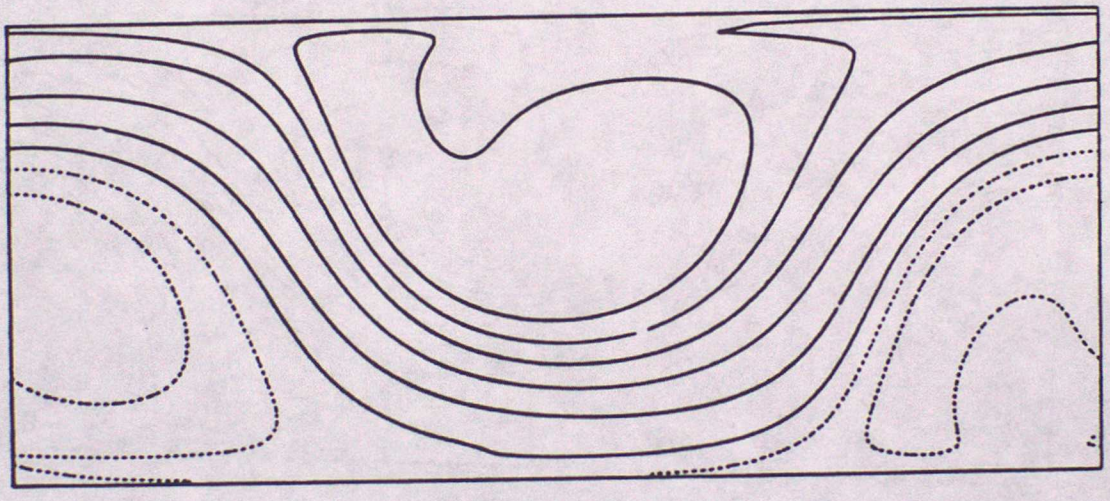

c

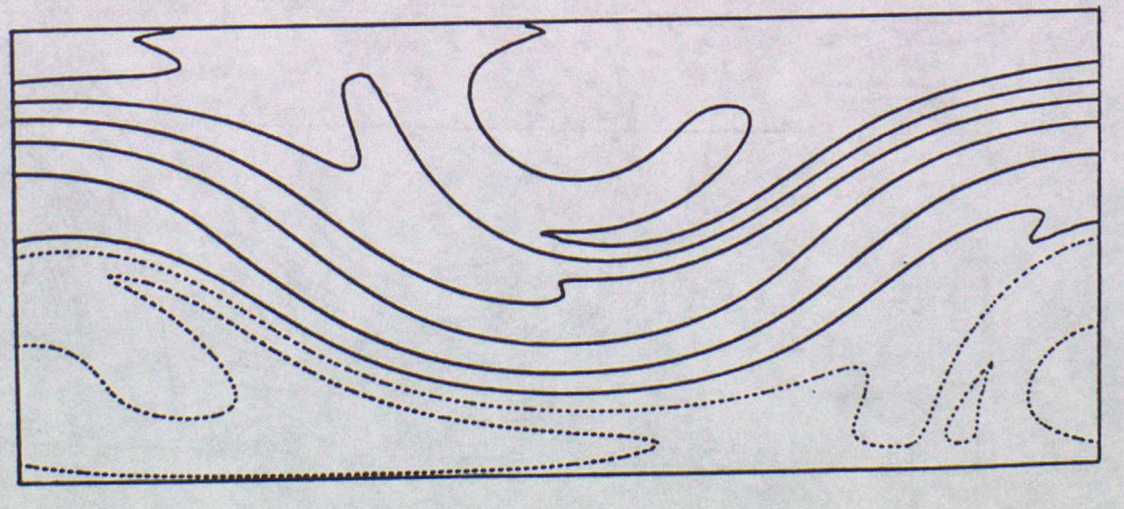

Figure 6

a

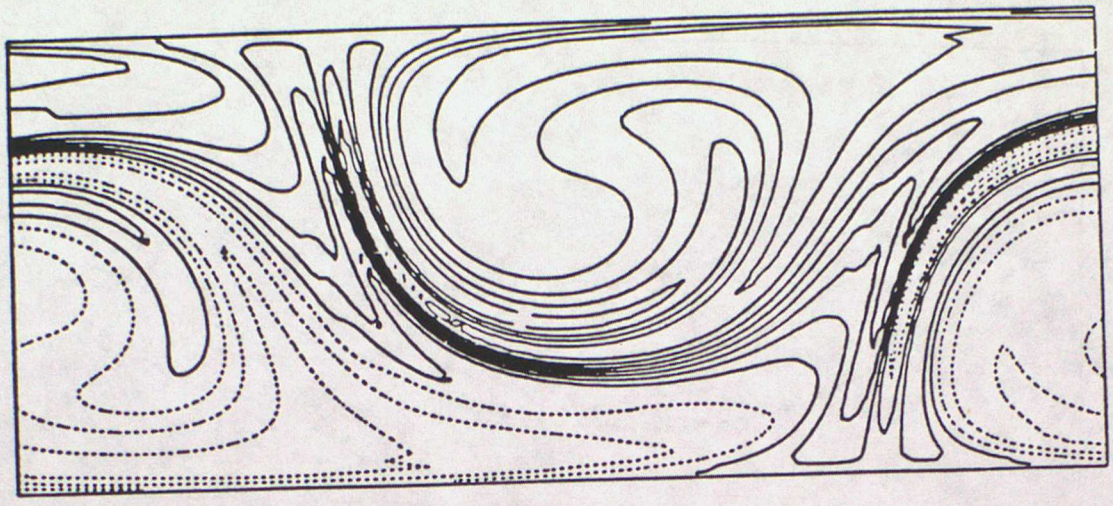

b

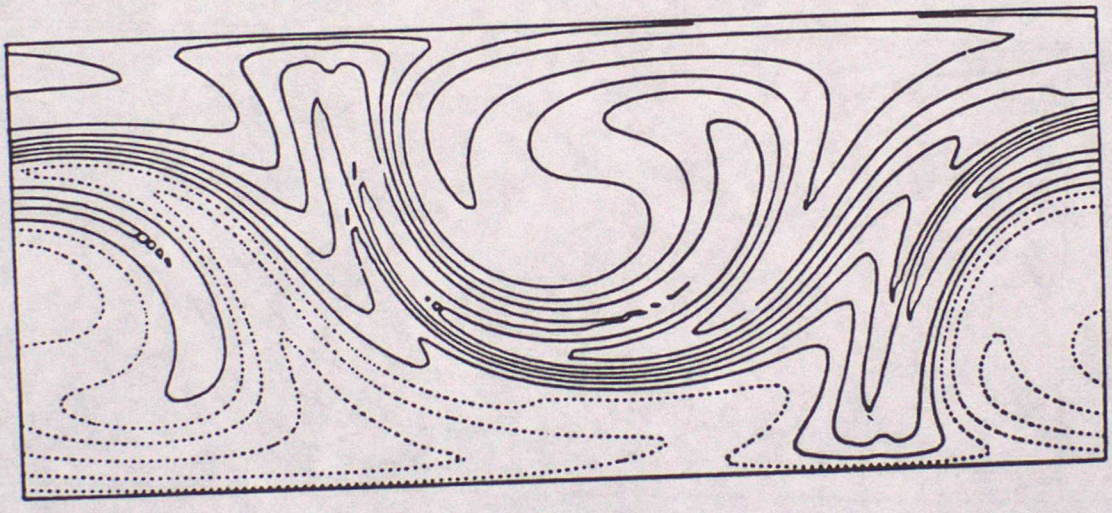

c

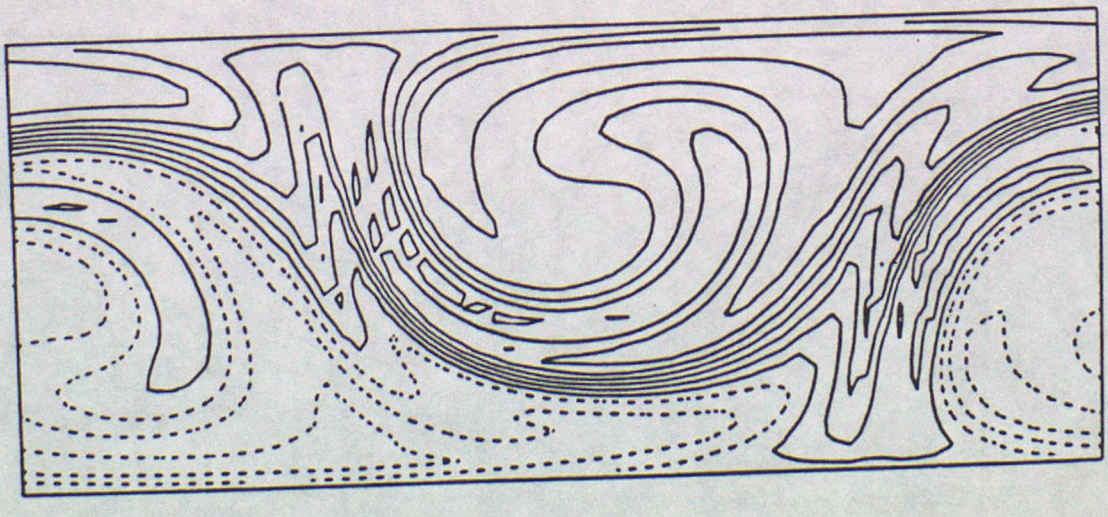

Figure 7

a

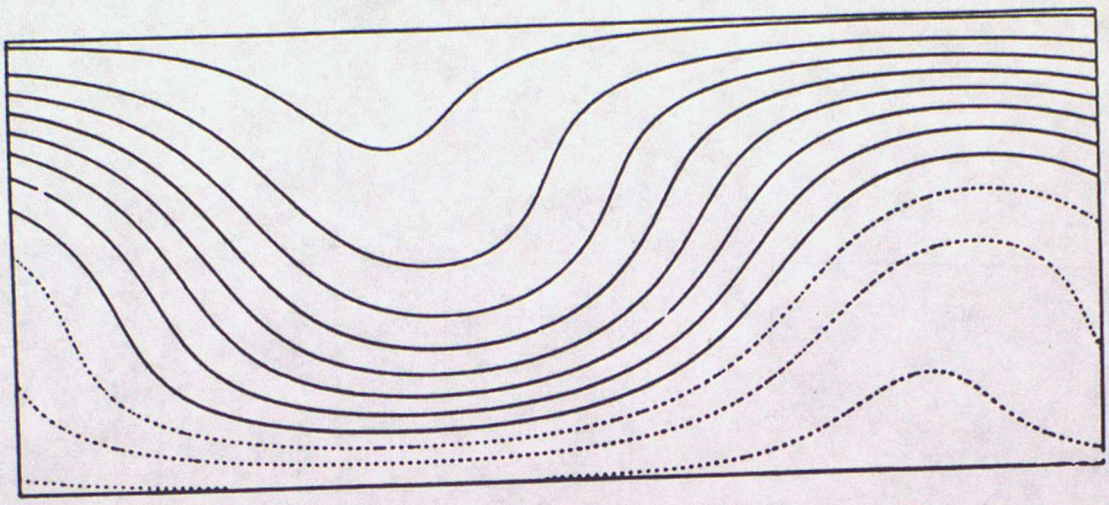

b

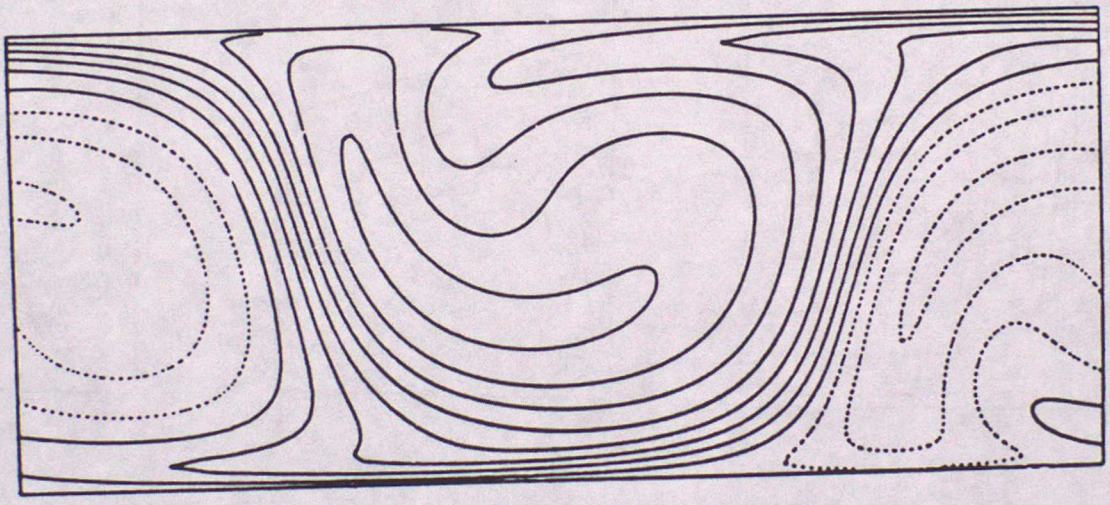

c

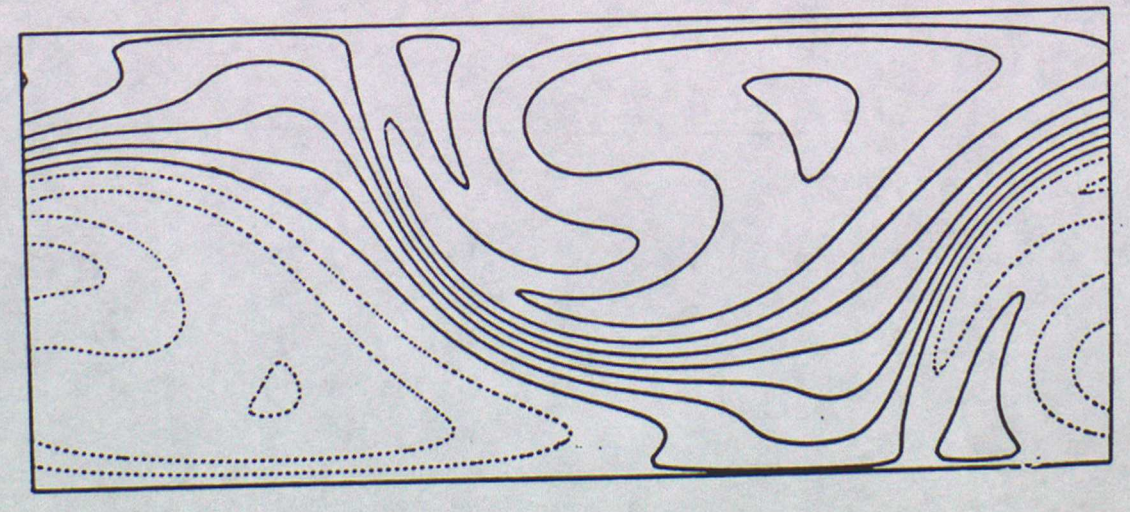

Figure 8

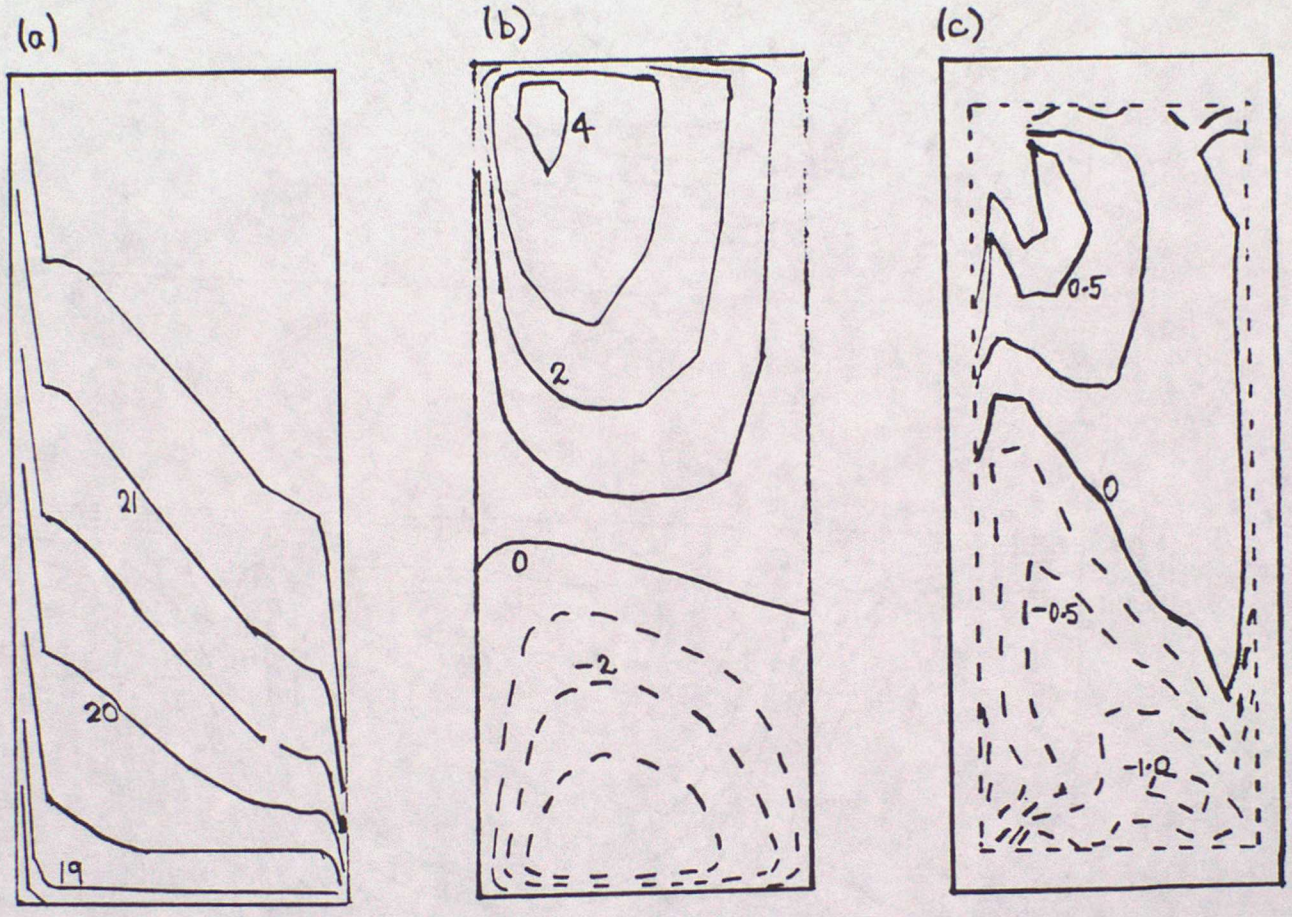

Figure 9

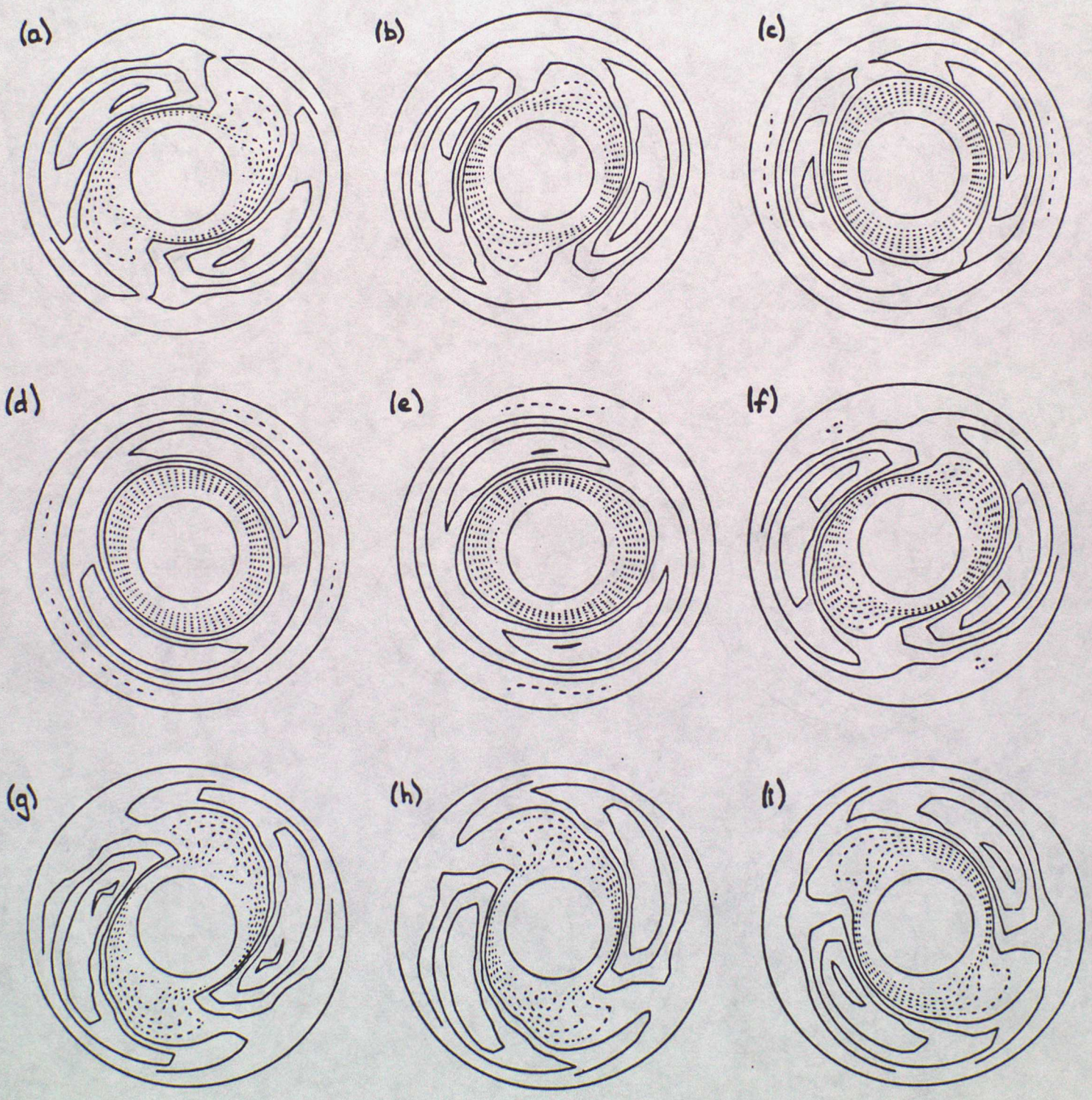

Figure 10

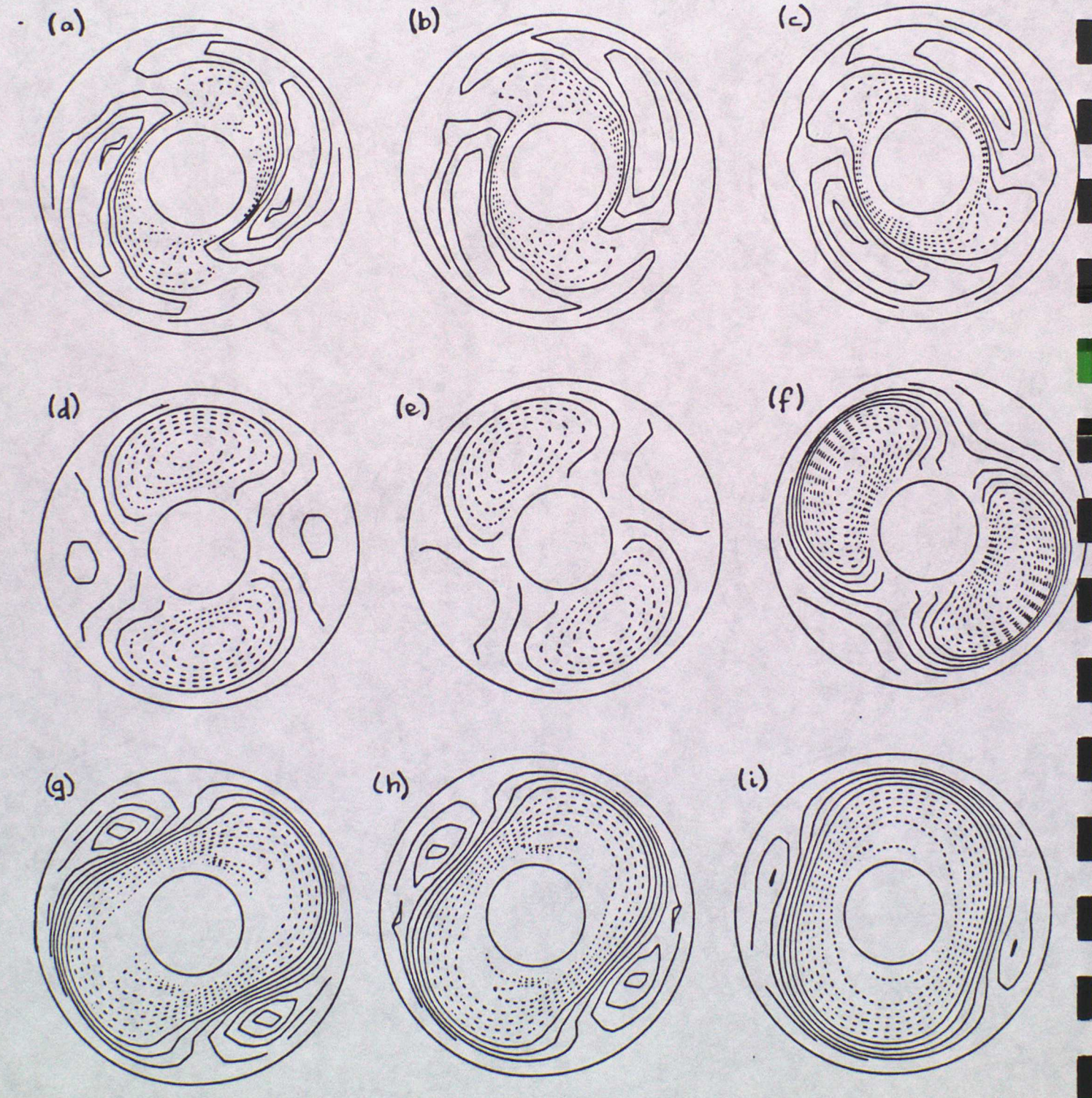

CURRENT SHORT - RANGE FORECASTING RESEARCH SCIENTIFIC NOTES (APRIL 1991)

The Short- Range Forecasting Research Branch (formerly Met O 11) Scientific Notes which contain information of current use are listed below. The complete set of Scientific Notes is available from the National Meteorological Library on loan, if required.

2. **Properties of the partial differential equations governing various types of atmospheric motions and implications for numerical methods.**
M.J.P. Cullen
December 1987

3. **A geometric model of balanced, axisymmetric flows with embedded penetrative convection.**
G.J. Shutts, M. Booth and J. Norbury
February 1988

4. **Implicit finite difference methods for computing discontinuous atmospheric flows.**
M.J.P. Cullen
March 1988

5. **Variational aspects of semi-geostrophic theory.**
R.J. Purser
August 1988

6. **On the incorporation of atmospheric boundary layer effects into a balanced model.**
M.J.P. Cullen
July 1988

7 **Implicit finite difference methods for modelling discontinuous atmospheric flows.**
M.J.P. Cullen
June 1988

8. **An analytical model of the growth of a frontal intrusion.**
M.W. Holt and G.J. Shutts
November 1988

9. **Planetary semi-geostrophic equations derived from Hamilton's principle.**
G.J. Shutts
July 1988

10. **Semi-geostrophic moist frontogenesis in a Lagrangian model.**
M.W. Holt
September 1988

11. **Generalised Lagrangian solutions for atmospheric and ocean flows.**
M.J.P. Cullen, J. Norbury and R.J. Purser
November 1988

12. **Properties of the Lagrangian semi-geostrophic equations.**
M.J.P. Cullen and R.J. Purser
January 1989

CURRENT SHORT - RANGE FORECASTING RESEARCH SCIENTIFIC NOTES (APRIL 1991) CONTINUED

13. **A simple two phase precipitation scheme for use in numerical weather prediction models.**
B.W. Golding
June 1989

14. **A test of a semi-implicit integration technique for a fully compressible non-hydrostatic model.**
M.J.P. Cullen
September 1989

15. **Dynamical aspects of the October storm 1987 : A study of a successful Fine-mesh simulation**
G.J. Shutts
September 1989

16. **A conservative split-explicit integration scheme suitable for forecast and climate models.**
M.J.P. Cullen and T. Davies
October 1989

17. **The dynamical structure of some North Atlantic depressions simulated by the fine-mesh model.**
G.J.Shutts
January 1990

18. **An Idealised Simulation of the Indian Monsoon using Primitive Equation and Quasi - Equilibrium models.**
M.H. Mawson and M.J.P. Cullen
August 1990

19. **Time - Integration Schemes for meteorological simulations involving oscillatory and dissipative modes.**
R.J. Purser
July 1990

20. **Mesoscale Model Experimental forecasts of the Haar of North East Scotland.**
S.P. Ballard, B.W.Golding, R.N.B. Smith
August 1990

21. **A conservative split-explicit integration scheme with fourth order horizontal advection.**
M.J.P. Cullen and T. Davies
October 1990

22. **A Geometric Model of the Nonlinear Equilibration of Two-Dimensional Eady Waves.**
M.J.P. Cullen and I. Roulstone
February 1991

23. **The Non-linear Evolution of a slowly growing wave on a laterally sheared baroclinic flow.**
M.J. Bell
April 1991